National Library
of Canada

Acquisitions and
Bibliographic Services Branch

395 Wellington Street
Ottawa, Ontario
K1A 0N4

Bibliothèque nationale
du Canada

Direction des acquisitions et
des services bibliographiques

395, rue Wellington
Ottawa (Ontario)
K1A 0N4

Your file Votre référence

Our file Notre référence

NOTICE

The quality of this microform is heavily dependent upon the quality of the original thesis submitted for microfilming. Every effort has been made to ensure the highest quality of reproduction possible.

If pages are missing, contact the university which granted the degree.

Some pages may have indistinct print especially if the original pages were typed with a poor typewriter ribbon or if the university sent us an inferior photocopy.

Reproduction in full or in part of this microform is governed by the Canadian Copyright Act, R.S.C. 1970, c. C-30, and subsequent amendments.

AVIS

La qualité de cette microforme dépend grandement de la qualité de la thèse soumise au microfilmage. Nous avons tout fait pour assurer une qualité supérieure de reproduction.

S'il manque des pages, veuillez communiquer avec l'université qui a conféré le grade.

La qualité d'impression de certaines pages peut laisser à désirer, surtout si les pages originales ont été dactylographiées à l'aide d'un ruban usé ou si l'université nous a fait parvenir une photocopie de qualité inférieure.

La reproduction, même partielle, de cette microforme est soumise à la Loi canadienne sur le droit d'auteur, SRC 1970, c. C-30, et ses amendements subséquents.

Canada

Tunability of photonic gaps in one and two dimensions

François Xavier Sezikeye

A Thesis

in

The Department

of

Physics

Presented in Partial Fulfillment of the Requirements

for the Degree of Master of Science at

Concordia University

Montreal, Quebec, Canada

January 1995

ISBN 0-612-01340-5

Canada

ABSTRACT

Tunability of photonic gaps in one and two dimensions

François Xavier Sezikeye

The transfer matrix method is used to evaluate the dispersion relation of electromagnetic (EM) waves propagating through complex systems in which the refractive index varies periodically along one dimension. The width and the position of the photonic gaps in this dispersion relation are shown to depend on the width, the refractive index, and the position of an additional structure in a conventional superlattice unit. In this way, certain gaps increase by a factor two to an order of magnitude, and others decrease when compared to the corresponding gaps of the unmodulated system, especially to that of a quarter-wave (QW) structure.

The transmittance of finite one-dimensional (1D) periodic structures is shown to follow closely the gap pattern when the number of units is sufficiently large. When the periodic arrangement is slightly changed to produce a Fibonacci chain, or a finite regular bi-layered structure with a missing layer, narrow allowed bands are introduced in the gaps. This leads to very few frequencies allowed to travel in a given medium.

Two-dimensional (2D) structures, with a refractive index that varies periodically along two dimensions are studied with plane wave methods. The gaps of the unmodulated system become larger or smaller, and sometimes vanish depending on the index and the dimensions of the added structure.

Dedicated to Minani, Rwasa, Pascaline, Bertrand-Olivier, and Delphine Jenny

ACKNOWLEDGMENTS

The author would like to express his gratitude to Prof. P. Vasilopoulos for proposing the subject of this study and following closely the development of the thesis. His suggestions of interesting seminars, papers and courses, and his questioning of every step undertaken and every result, were crucial to the successful accomplishment of this work.

The author is also indebted to Dr. R. Akis for his numerous advices in numerical problems and for his every day's availability.

Further, the author wishes to express his gratitude to the faculty and the staff of the Physics Department, especially to Profs. N. Eddy and J. Shin for having always their door open.

Finally, the author appreciates the friendship of his graduate fellows who were always willing to share their latest shortcut to different tasks.

TABLE OF CONTENTS

LIST OF FIGURES

LIST OF TABLES

CHAPTER 1

INTRODUCTION

1.1 Historical review

Without going as far as Abelès' works[1] on transmission of electromagnetic waves in thin layers in 1948, the study of gaps in periodic media can be retraced to the works Bykov[42] on the effect of a one-dimensionsional (1D) periodicity on the spontaneous emission in the mid 70's. Since then, a tremendous progress has been made in the study of 1D systems, following the works of Yariv[45] and van der Ziel[48]. The localization of light and the photonic gaps in two and three dimensions have been investigated since the mid 80's, especially by Yablonovich[42], John[32, 31], Soukoulis[49], Leung[20], etc... At the same time, several transmission experiments have been conducted by Smith[35] and McCall[26].

One of the most important applications of periodic structures is the Bragg reflection in semiconductor lasers. The first lasers with 1D Bragg reflectors were realized in 1975[29]. Nowadays, reflectances as high[41] as 0.9995 are common in the industries. Investigations on 2D Bragg reflectors[6] in the early '90 suggest that they will soon replace the 1D reflectors in 1D laser diode arrays, and that 3D reflectors will be coupled to 2D laser diode arrays. Another application of the photonic gaps is the thresholdless lasers which appeared in 1988[7].

The analogy between electrons and photons in periodic structures was first noticed by D. Kossel[19] in 1966, and since then, the methods used in these two fields are very similar. Similar to electrons in crystal, light propagation in media whose refractive index varies periodically, is associated with allowed and forbidden bands. The latter are called photonic gaps.

1.2 Motivation

The existence of photonic gaps has been found very usefull especially with the realization of the Bragg reflectors used in semiconductor lasers. The lasing cavity[41] must effectively eliminate any undesired frequency that would just produce heat, lower the efficiency of the system, and even destroy the semiconductor. In addition, the operating frequency of the laser must be greatly reflected, so that every photon induce the emission of several other in-phase photons, thus reaching more easily the lasing threshold energy[42, 6, 38]. Here, the photonic gap which is responsible for the reflection must be centered on the desired frequency and it must be narrow.

Sometimes, photonic gaps are used to let some frequencies pass and stop others, for instance in a medium where spontaneous light emission occurs, or in a filter[9, 27, 43]. In all cases, the gap width must be specified. In real life, a high reflectance that can be obtained by a finite periodic structure is sufficient. Here it is crucial to obtain the same reflectance with fewer elements.

Photonic gaps do not appear necessarily at the frequency range where they are most needed and they do not always have the optimum bandwidth. The present work investigates methods that can tune the gaps and the reflectance to specific values.

1.3 Photonic gaps

When waves travel through a periodic potential, some frequency bands are not allowed. The word "potential" stands for a certain propagation characteristic of the considered wave. Gaps have been found to occur for electronic[25], electromagnetic[45] and acoustic[8] waves. The corresponding "potential" is the electric potential, the refractive index (or the dielectric constant), and the bulk modulus, respectively. As an example, the time-independent Schrödinger equation for an electron in a 1D periodic potential V(x)=V(x+a), and the corresponding electromagnetic wave equation in a medium with a periodic refractive index n(x)=n(x+a), are, respectively,

$$\nabla^2\psi + 2m\left(\frac{2\pi}{h}\right)^2(E - V(x))\psi = 0, \qquad 1.01$$

and

$$\nabla^2\varphi + n^2(x)\varphi = 0. \qquad 1.02$$

As can be seen above, Eqs. 1.01 and 1.02 are similar and one expects further analogies between their respective solutions.

The phenomenon of forbidden bands has been thoroughly studied for electrons in crystals where they are known to occupy definite energy bands. The electronic band structure of a crystal determines if the element is a metal, a semiconductor or an insulator. The generalization of the gap notion to electromagnetic waves suggests that the equivalent of a photonic semiconductor can be made, with possibilities of donor and acceptor levels in the gap. Even if some success has been claimed in the study of photonic gaps, no equivalent of the known semiconductor devices has been produced up to now.

Research in semiconductors has introduced the term "band gap engineering" as it underlines the various methods developed to tailor the semiconductor gaps to specific values suitable for applications. In semiconductor superlattices, a method has been proposed for tuning the minigaps by Peeters and Vasilopoulos[28] and by Vasilopoulos[37] et al. in more detail. It consists in adding barriers at the centers of the wells and it exploits the properties of the corresponding electronic wave function to move the minibands in the desired direction.

Until now, in photonic gap studies, only simple periodic structures have been analyzed[45 23], such as those shown in Figs. 1.1 and 1.2. Even in three dimensions[36], this was the rule. In the present approach, the nth unit of Fig. 1.1 is modified as shown in Fig. 1.2, for example.

So far, the reported photonic gaps are very small, about 1.15 Ghz [23]. One of the problems in this field is the modulation of the photonic gap. As we are not aware of any proposed modulation method, we study the change of the photonic gap bandwidth obtained by changing the structure of the periodic unit in analogy with electronic superlattices[37]. The idea is that a more frequent dielectric contrast in the unit leads to multiple destructive or constructive reflections of the waves and thus to an increase or decrease of the gaps. The same idea can be applied to the two-dimensional system of Fig. 1.3 and will be detailed later.

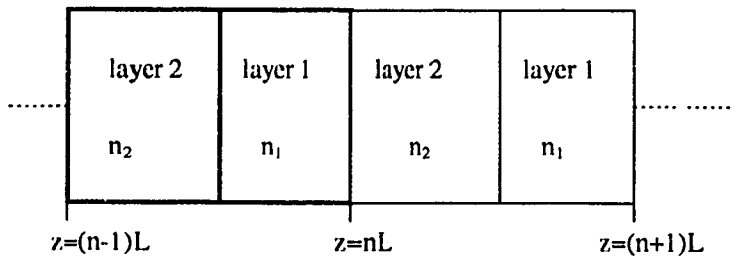

Fig. 1.01 Simple 1D two-layered superlattice; n_1 and n_2 are the refractive indices of the two layers.

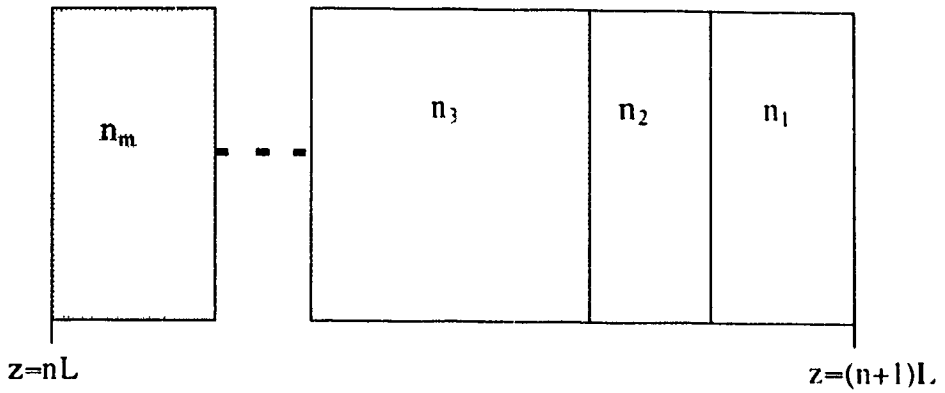

Fig.1.02: Possible 1-D multilayered unit

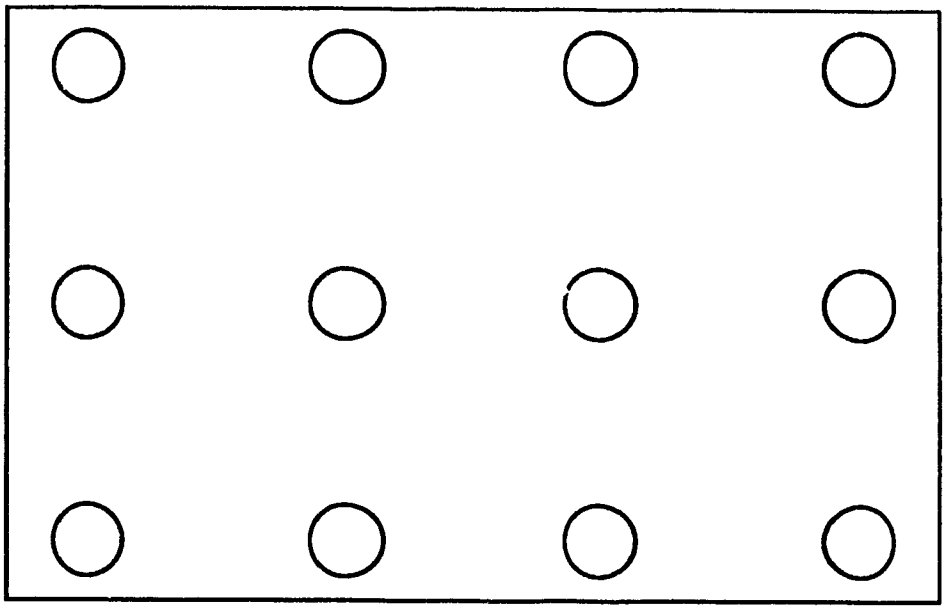

Fig. 1.03 Simple 2D structure. The shaded circles have a refractive index different from that of the background.

1.4 Outline

The work is organized as follows. In chapter 2, we give the dispersion relation for 1D periodic structures in analytic form. Maxwell's equations and the boundary conditions at the interfaces separating adjacent layers, are used to find the transfer matrix that links the electromagnetic wave's magnitude and phase in one unit to those of the following unit. This matrix contains the information on the forbidden and allowed frequencies. The gap position and width are studied as a function of the angle of incidence, the layers' thickness, the refractive indices, and the complex structure in the basic units. The results of these modifications are compared to the photonic gaps of a quarter-wave (QW) stack characterized by two layers with the same optical length per unit.

In chapter 3, we study finite structures, where the most interesting feature is the transmittance or transmittivity. Numerical results are obtained for QW finite structures, complex structures, pseudoperiodic structures such as Fibonacci chains, and structures with defects. Defects introduce narrow allowed bands in gaps. Where experimental results are available, they match closely the numerical results.

Chapter 4 deals with the tunability of the photonic gap in 2D structures; in a square lattice of cylinders or prisms, cylinders or prisms with different dimension and/or index are added to the unit and the photonic gaps are compared to those of structures with no interstitial elements. The transfer-matrix technique[34]

is not used here, as the plane-wave method is simpler to implement. Again the polarizations of the electromagnetic waves (TE and TM) are considered separately. Some conclusions are very similar to those pertaining to 1D structures, such as the maximum gap etc...

The fifth chapter analyzes possible applications of tuned gaps, what can further be done, and gives the conclusions.

Chapter 2

PHOTONIC GAPS IN 1D SUPERLATTICES

2.1 Superlattice description

A 1D superlattice is a layout of two or more parallel layers of different refractive indices, repeated in a periodic pattern. The most favorite material consists of a GaAs layer followed by a $Ga_{1-x}Al_xAs$ layer because of their matching lattice parameters[50] and their flexibility in varying their indices by choosing a suitable concentration x. The refractive index can vary from 2.97 for AlAs up to 3.59 for GaAs[38, 2] for the energies around 1.6 eV. It is given by

$$n_{Ga(1-x)Al(x)As} = 3.59 - 0.71x + 0.091x^2 \qquad 2.01$$

The lateral dimensions are supposed to be infinite, and the index varies only in the z direction. The most general form of the index pattern of our superlattice is shown in Fig. 2.01. If, for instance, the widths d_1 and d_n are the only ones to be different from zero, we have a two-layered structure. We assume that we have a certain liberty in choosing the magnitude of the widths d_i and the indices. However, in practice, it would be very difficult to collate too thin layers if

their indices are very different.

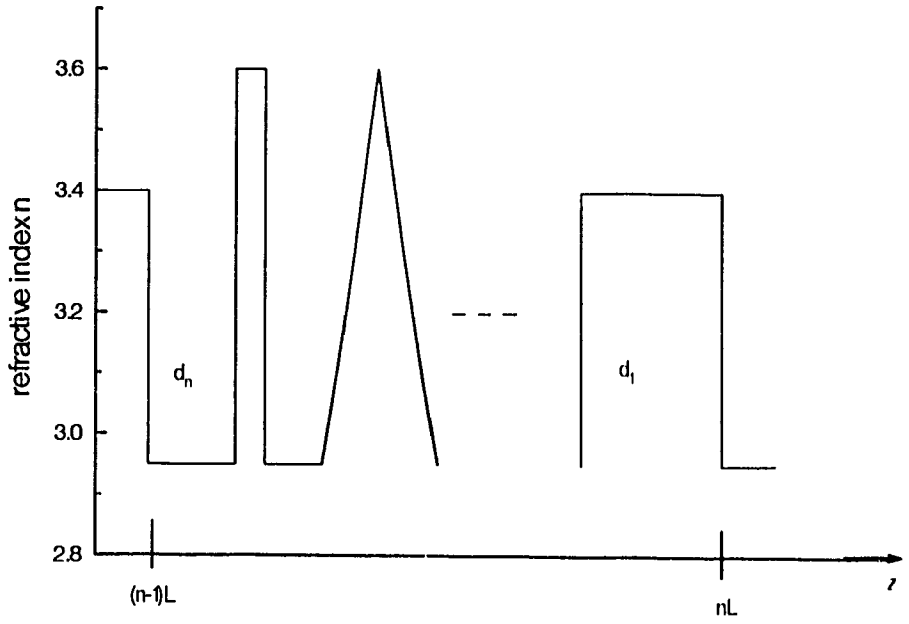

Fig. 2.01 Possible refractive index profile within one unit

2.2 Transfer matrices

A periodic structure with layers of different refractive indices exhibits gaps of energy in which no electromagnetic waves can propagate. For 1D structures, one of the ways of finding these photonic gaps is the use of the transfer matrix method[45] as it has been used in semiconductor superlattices for electrons[37]. The transfer matrix links the field amplitudes $A_{1(n-1)}$ and $B_{1(n-1)}$ in the

first layer of the (n-1)th unit to A_{1n} and B_{1n} in the first layer of the nth unit, as shown in Fig. 2.02.

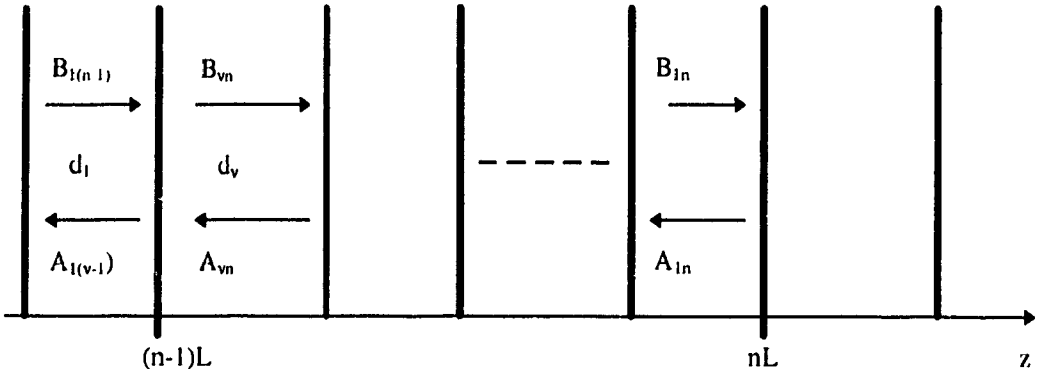

Fig. 2.02 EM waves in one unit

The most general case consists of an infinite chain of similar units, with v layers in each unit. Each layer has its own refractive index and width, and the z-axis is chosen to be perpendicular to its faces. The overall width of the unit is the period L.

Let us consider the electromagnetic field in the mth layer of the nth unit. The most general electromagnetic wave is a sum of two waves, the transverse electric (TE) and the transverse magnetic (TM) waves, which can be studied separately. The TE wave has its *electric* field $\vec{E}$ perpendicular to the plane of incidence, in the present case, the yz plane, whereas the TM wave has the *magnetic* field $\vec{H}$ perpendicular to the plane of incidence.

In the present investigation, we only consider lossless and non magnetic (μ=1) layers. In such a case, Maxwell's equations read

$$\nabla \times \vec{E} = -\frac{\partial \vec{H}}{\partial t} \quad , \qquad 2.02$$

$$\nabla \times \vec{H} = \varepsilon \frac{\partial \vec{E}}{\partial t}, \qquad 2.03$$

$$\nabla \bullet \vec{E} = 0, \qquad 2.04$$

$$\nabla \bullet \vec{H} = 0. \qquad 2.05$$

These equations can be combined to give the wave equations for $\dot{E}$ and $\dot{H}$.

$$\nabla \times \nabla \times \vec{E} + \varepsilon \frac{\partial^2 \vec{E}}{\partial t^2} = 0, \qquad 2.06$$

$$\nabla \times \left(\frac{1}{\varepsilon} \nabla \times \vec{H} \right) + \frac{\partial^2 \vec{H}}{\partial t^2} = 0. \qquad 2.07$$

The solutions of the wave equations are sums of forward and backward waves; in the mth layer of the nth unit, they read

$$E(y,z,t) = E(y,z)e^{i\omega t} = \left(A_{mn} e^{ik_{mz}(z - nL)} + B_{mn} e^{-ik_{mz}(z - nL)} \right) e^{i(k_y y - \omega t)} \quad , \qquad 2.08$$

$$H(y,z,t) = H(y,z)e^{-i\omega t} = \left(C_{mn} e^{ik_{mz}(z - nL)} + D_{mn} e^{-ik_{mz}(z - nL)} \right) e^{i(k_y y - \omega t)} \quad . \qquad 2.09$$

The wave vector component along the z axis, k_{zm}, is given by

$$k_{mz} = \frac{n_m \omega}{c} \cos\theta_m, \qquad 2.10$$

where ω is the electromagnetic frequency, n_m the refractive index of the mth layer, θ_m the angle of incidence, and c the velocity of light in vacuum.

Maxwell's equations will help solving the boundary problem at interfaces[16, 14, 4]. The fields have to be continuous at the interfaces, or if we consider the electric (magnetic) field only, the field and its first derivative[45] with respect to z (E_x and $\partial E_x/\partial z$ or H_x and $\partial H_x/\partial z$) must be continuous. For the electric fields, this translates into the following equations in layers m and m+1, with subscript s for TE waves and p for TM waves:

$$E_{ism} + E_{rsm} = E_{is(m+1)} + E_{rs(m+1)} \quad , \tag{2.11}$$

$$\left(-E_{ism} + E_{rsm}\right) n_m \cos\theta_m = \left(-E_{is(m+1)} + E_{rs(m+1)}\right) n_{(m+1)} \cos\theta_{(m+1)} \quad , \tag{2.12}$$

$$\left(E_{ipm} + E_{rpm}\right) \cos\theta_m = \left(E_{ip(m+1)} + E_{rp(m+1)}\right) \cos\theta_{(m+1)} \quad , \tag{2.13}$$

$$\left(-E_{ipm} + E_{rpm}\right) n_m = \left(-E_{ip(m+1)} + E_{rp(m+1)}\right) n_{(m+1)} \quad . \tag{2.14}$$

Combinations of Eqs. 2.08 to 2.09 and 2.11 to 2.14 give the relation between the electric field amplitudes in adjacent layers. From the last layer of the (n-1)th unit to the first layer of the nth unit, cf. Fig. 2.02, the matrix form of the boundary conditions for TE waves reads

$$\begin{pmatrix} 1 & 1 \\ -k_{1z} & k_{1z} \end{pmatrix} \begin{pmatrix} A^1_{n-1} \\ B^1_{n-1} \end{pmatrix} = \begin{pmatrix} e^{ik_{vz}L} & e^{-ik_{vz}L} \\ -k_v e^{ik_{vz}L} & k_v e^{-ik_{vz}L} \end{pmatrix} \begin{pmatrix} A^v_n \\ B^v_n \end{pmatrix} . \tag{2.15}$$

For TM waves we obtain

$$\begin{pmatrix} \frac{k_{1z}}{n_1} & \frac{k_{1z}}{n_1} \\ -n_1 & n_1 \end{pmatrix} \begin{pmatrix} A^1_{n-1} \\ B^1_{n-1} \end{pmatrix} = \begin{pmatrix} \frac{k_{vn}}{n_v} e^{ik_{vz}L} & \frac{k_{vn}}{n_v} e^{-ik_{vz}L} \\ -n_v e^{ik_{vz}L} & n_v e^{-ik_{vz}L} \end{pmatrix} \begin{pmatrix} A^v_n \\ B^v_n \end{pmatrix} . \qquad 2.16$$

Between two adjacent layers of the *same* unit j and j+1, j going from 1 to ν-1, the transfer matrices for TE and TM waves are as follows

$$\begin{pmatrix} e^{ik_{jz}\Lambda_j} & e^{-ik_{jz}\Lambda_j} \\ -k_{jz}e^{ik_{jz}\Lambda_j} & k_{jz}e^{-ik_{jz}\Lambda_j} \end{pmatrix} \begin{pmatrix} A^j_n \\ B^j_n \end{pmatrix} = \begin{pmatrix} e^{ik_{(j+1)z}\Lambda_j} & e^{-ik_{(j+1)z}\Lambda_j} \\ -k_{(j+1)z}e^{ik_{(j+1)z}\Lambda_j} & k_{(j+1)z}e^{-ik_{(j+1)z}\Lambda_j} \end{pmatrix} \begin{pmatrix} A^{j+1}_n \\ B^{j+1}_n \end{pmatrix}, \qquad 2.17$$

and

$$\begin{pmatrix} \frac{k_{jz}}{n_j}e^{ik_{jz}\Lambda_j} & \frac{k_{jz}}{n_j}e^{-ik_{jz}\Lambda_j} \\ -n_j e^{ik_{jz}\Lambda_j} & n_j e^{-ik_{jz}\Lambda_j} \end{pmatrix} \begin{pmatrix} A^j_n \\ B^j_n \end{pmatrix} = \begin{pmatrix} \frac{k_{(j+1)z}}{n_{j+1}}e^{ik_{(j+1)z}\Lambda_j} & \frac{k_{(j+1)z}}{n_{j+1}}e^{-ik_{(j+1)z}\Lambda_j} \\ -n_{j+1}e^{ik_{(j+1)z}\Lambda_j} & n_{j+1}e^{-ik_{(j+1)z}\Lambda_j} \end{pmatrix} \begin{pmatrix} A^{j+1}_n \\ B^{j+1}_n \end{pmatrix}, \qquad 2.18$$

where

$$\Delta_i = \sum_{j=1}^{j=i} d_j . \qquad 2.19$$

Here, d_j is the width of the jth layer. By matrix manipulations, one easily finds the transfer matrix M that links the amplitudes of the electric fields in two adjacent units. For the (n-1)th and the nth unit we have

$$\begin{pmatrix} A^1_{n-1} \\ B^1_{n-1} \end{pmatrix} = M \begin{pmatrix} A^1_n \\ B^1_n \end{pmatrix} . \qquad 2.20$$

M is a 2x2 matrix and has the properties

$$M_{11} = M_{22}^{*} \quad , \qquad M_{12} = M_{21}^{*} \; ; \tag{2.21}$$

where * denotes the complex conjugate of the element considered. Thus, two matrix elements are sufficient to define the matrix M. If 2EM, 3EM, 4EM designate the transfer matrices of two, three, and four-layered units for TE waves, and 2MM, 3MM, 4MM the equivalent matrices for TM waves, the matrix elements for TE waves are found to be

$$\begin{aligned} 2EM_{11} = \frac{1}{2^2 k_{1z} k_{2z}} \{ & (k_{1z} + k_{2z})(k_{2z} + k_{1z}) \exp[i(k_{2z} d_2 + k_{1z} d_1)] \\ & + (k_{1z} - k_{2z})(k_{2z} - k_{1z}) \exp[i(-k_{2z} d_2 + k_{1z} d_1)] \} \end{aligned} \quad , \tag{2.22}$$

and

$$\begin{aligned} 2EM_{21} = \frac{1}{2^2 k_{1z} k_{2z}} \{ & (k_{1z} - k_{2z})(k_{2z} + k_{1z}) \exp[i(k_{2z} d_2 + k_{1z} d_1)] \\ & + (k_{1z} + k_{2z})(k_{2z} - k_{1z}) \exp[i(-k_{2z} d_2 + k_{1z} d_1)] \} \end{aligned} \quad . \tag{2.23}$$

The corresponding equations for $4EM_{ij}$ with which most of the calculations have been carried out are very complicated. To simplify their form, we introduce the notation

$$\begin{aligned} & k_{iz} + k_{jz} = k_{ij} \quad , \quad k_{iz} - k_{jz} = \bar{k}_{ij}, \\ & \frac{n_i^2}{k_{iz}} + \frac{n_j^2}{k_{jz}} = q_{ij} \quad , \quad \frac{n_i^2}{k_{iz}} - \frac{n_j^2}{k_{jz}} = \bar{q}_{ij}, \end{aligned} \tag{2.24}$$

$$R_{ijkl} = \exp\left[i\left(k_{iz}d_i + k_{jz}d_j - k_{kz}d_k + k_l d_l \cdots\right)\right]. \qquad 2.25$$

Then we have

$$\begin{aligned} 4EM_{11} = & \frac{1}{2^4 k_{4z}k_{3z}k_{2z}k_{1z}} \\ & \left\{k_{14}k_{43}k_{32}k_{21}R_{4321} + \bar{k}_{14}\bar{k}_{43}k_{32}k_{21}R_{4321} + \bar{k}_{14}k_{43}\bar{k}_{32}k_{21}R_{4321}\right. \\ & + \bar{k}_{14}k_{43}k_{32}\bar{k}_{21}R_{4321} + k_{14}\bar{k}_{43}\bar{k}_{32}k_{21}R_{4321} + k_{14}\bar{k}_{43}k_{32}\bar{k}_{21}R_{4321} \\ & \left. + k_{14}k_{43}\bar{k}_{32}\bar{k}_{21}R_{4321} + \bar{k}_{14}\bar{k}_{43}\bar{k}_{32}\bar{k}_{21}R_{4321}\right\}, \end{aligned} \qquad 2.26$$

and

$$\begin{aligned} 4EM_{21} = & \frac{1}{2^4 k_{4z}k_{3z}k_{2z}k_{1z}} \\ & \left\{\bar{k}_{14}k_{43}k_{32}k_{21}R_{4321} + k_{14}\bar{k}_{43}k_{32}k_{21}R_{4321} + k_{14}k_{43}\bar{k}_{32}k_{21}R_{4321}\right. \\ & + k_{14}k_{43}k_{32}\bar{k}_{21}R_{4321} + \bar{k}_{14}\bar{k}_{43}\bar{k}_{32}k_{21}R_{4321} + \bar{k}_{14}\bar{k}_{43}k_{32}\bar{k}_{21}R_{4321} \\ & \left. + \bar{k}_{14}k_{43}\bar{k}_{32}\bar{k}_{21}R_{4321} + k_{14}\bar{k}_{43}\bar{k}_{32}\bar{k}_{21}R_{4321}\right\}. \end{aligned} \qquad 2.27$$

All the matrix elements αMM_{ij} can be obtained from the matrix elements of αEM_{ij} upon replacing k_j by n_j^2/k_{jz}. The most important quantity in the matrix elements is the ratio between adjacent layers' indices.

2.3 Dispersion relation

The transfer matrix M between two corresponding layers of adjacent units can be used to link similar layers belonging to any two units of the structure by means of in Eq. 2.28.

$$\begin{pmatrix} A_0^l \\ B_0^l \end{pmatrix} = M^n \begin{pmatrix} A_n^l \\ B_n^l \end{pmatrix}. \qquad 2.28$$

In physical problems, we expect M^n to be finite even when n goes to infinity. In other words, the absolute value of its determinant must be equal to or inferior to one. When the layers are lossless, as they are in our case, the determinant is equal to one, and the matrix M is called unimodular[45]. Its eigenvalues are found by solving the following equation.

$$M\begin{pmatrix} A_n \\ B_n \end{pmatrix} = p\begin{pmatrix} A_n \\ B_n \end{pmatrix} \Leftrightarrow (M - pI)\begin{pmatrix} A_n \\ B_n \end{pmatrix} = 0\,. \qquad 2.29$$

Equation 2.29 shows that the determinant of (M-pI) is equal to zero, with I standing for the identity matrix. With det (M)=$M_{11}M_{22}$-$M_{12}M_{21}$=1, Eq. 2.29 can be solved and the eigenvalues p be found as follows;

$$\begin{aligned} \det(M - pI) &= (M_{11} - p)(M_{22} - p) - M_{11}M_{21} \\ &= p^2 - p(M_{11} + M_{22}) + 1 \\ &= p^2 - p\,\mathrm{tr}(M) + 1 = 0. \end{aligned} \qquad 2.30$$

This gives

$$p_{\pm} = \frac{\mathrm{tr}M \pm \sqrt{\mathrm{tr}^2 M - 4}}{2}. \qquad 2.31$$

Equation 2.28 can now be written as follows

$$\begin{pmatrix} A_0 \\ B_0 \end{pmatrix} = M^n \begin{pmatrix} A_n \\ B_n \end{pmatrix} = p^n \begin{pmatrix} A_n \\ B_n \end{pmatrix}. \qquad 2.32$$

Again, the condition of a finite value when n goes to infinity prescribes a solution of the form

$$\left|p^n\right| = 1 \quad \Leftrightarrow \quad p = e^{\pm iKL}. \qquad 2.33$$

The combination of Eqs. 2.31 and 2.33 gives a condition of existence of any wavelength in the periodic structure, i.e. the dispersion relation

$$\cos(KL) = \mathrm{tr}M/2. \qquad 2.34$$

In fact, any wavelength that will yield a value of cos(KL) superior to 1 or inferior to -1 will not propagate in the medium. Thus, the study of band gaps is reduced to the calculation of the trace of the matrix M, and if we take into account Eq. 2.21, the matrix element M_{11} is sufficient. Then, we can say that only frequencies that fulfill the condition $-1 \le \mathrm{tr}(M)/2 = \mathrm{Real}(M_{11}) \le 1$, can propagate through the superlattice.

The analysis of M_{11} in Eqs. 2.22 to 2.27 suggests that the contrast of adjacent refractive indices will determine the width of the gap by giving to the real part of M_{11} a value out of the physical limits. The index of each layer is coupled to that of its neighbors, an absence of contrast will lead to an absence of contribution of terms containing the difference of the indices. A large contrast will lead to an important contribution in a negative or a positive way thus maintaining the trace below -1 or above 1 and making the gap larger.

For a two-layered structure, the dispersion relations for TE and TM waves are respectively given by

$$\cos(KL) = \cos(k_{1z}d_1)\cos(k_{2z}d_2) - \frac{1}{2}\left(\frac{k_{1z}}{k_{2z}} + \frac{k_{2z}}{k_{1z}}\right)\sin(k_{1z}d_1)\sin(k_{2z}d_2), \qquad 2.35$$

and

$$\cos(KL) = \cos(k_{1z}d_1)\cos(k_{2z}d_2) - \frac{1}{2}\left(\frac{n_1^2k_{2z}}{n_2^2k_{1z}} + \frac{n_2^2k_{1z}}{n_1^2k_{2z}}\right)\sin(k_{1z}d_1)\sin(k_{2z}d_2). \qquad 2.36$$

The frequency dependence of the equations above is shown in Fig. 2.03 for a angle of incidence equal to 0.5 rad.

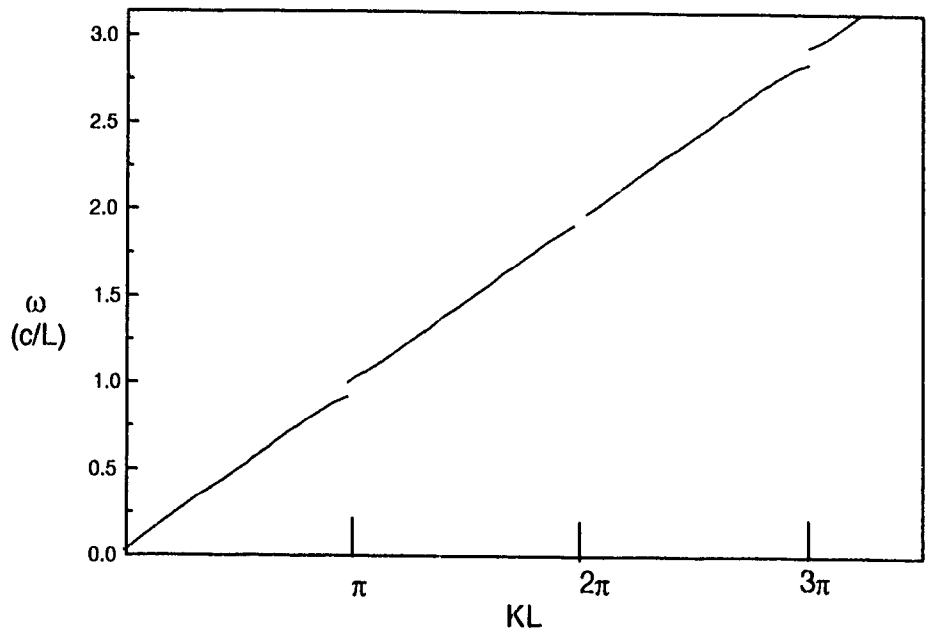

Fig. 2.03 Dispersion relation ω vs KL. The discontinuities at KL=nπ, n=1,2,3 represent the first, second and third photonic gaps, respectively.

2.4 Numerical results

Up to now, the superlattice structures that are found in the literature are made of two layers different in width and refractive index[45, 10, 12, 42.]. We will insert an extra layer in one of these two layers and study if the gaps vanish, widen or shrink when the width and the refractive index of the extra layer vary. Further, we will see the sort of gap we can get if the index varies spatially in a more complex fashion, for instance, in a triangular pattern.

The basic two-layered structure considered here is the QW stack in which the optical path OP = Width*Index is the same for each layer. In this particular case, the middle of the band gaps ω_i and the gap width $\Delta\omega_i$ are easily deduced analytically[45] from Eqs. 2.35 and 2.36, with KL=nπ+ix corresponding to gaps. If we assume a normal incidence, we obtain

$$\omega_i = \frac{\pi c i}{2 d_1 n_1}, \qquad 2.37$$

and

$$\Delta\omega_i = \begin{cases} 4\omega_i \dfrac{n_1 - n_2}{\pi(n_1 + n_2)}, & i = 1, 3, 5... \\ 0, & i = 2, 4, 6... \end{cases} \qquad 2.38$$

That is, all even-numbered gaps vanish identically. By considering that gaps are created by the buildup of successive reflections, we can easily see why only odd gaps are present under normal incidence for a QW structure. When an electromagnetic wave is reflected by an interface separating a low index medium from a high index medium, the reflected wave is 180° out of phase with respect to the incident one[4]. Hence, a wave, with length equal to a quarter of the optical width of a QW layer, that travels through a QW unit and back, will be in phase with the wave reflected by the first interface of the unit. On the other hand, a wavelength equal to twice the optical length of the QW layers will interfere destructively with the wave reflected from the previous unit thus preventing the reflections to build up.

Let us take a QW structure made of two layers of $Ga_{1-x}Al_xAs$ with different values of x such that the indices are equal to 3.59 and 3 for widths equal to 90 nm and 107.7 nm, respectively. The z axis is perpendicular to the layers. According to Eqs. 2.39 and 2.40, gaps are expected at odd multiples of ω_0 for an angle of incidence equal to zero with

$$\omega_0 = 1.46\ 10^{15}\ \text{rd/s}, \qquad 2.39$$

$$\Delta\omega = 0.228\,\omega. \qquad 2.40$$

All gaps are equal in magnitude, thus their relative width with respect to the middle of the gap gets smaller and smaller for higher gaps. As the ratio $\Delta\omega/\omega$ is the quantity that often matters in experiments, there is practically no gap at high

frequencies. Anyway, it would not be realistic to go far beyond the first gap energy because the indices will change with the energy. So, at twice the first QW midgap, the index ratio for adjacent layers jumps from 0.7 to 0.8 according to Afromowitz [2], and the transfer matrix has no longer the same eigenvalues.

A more practical unit for ω is c/L where c is the velocity of light in vacuum and L the width of one unit. If the angle of incidence θ varies from 0 to $\pi/2$, k_z and k_y will change accordingly and the use of the transfer matrix method yields the results shown in Fig. 2.04 for TE waves and in Fig. 2.05 for TM waves.

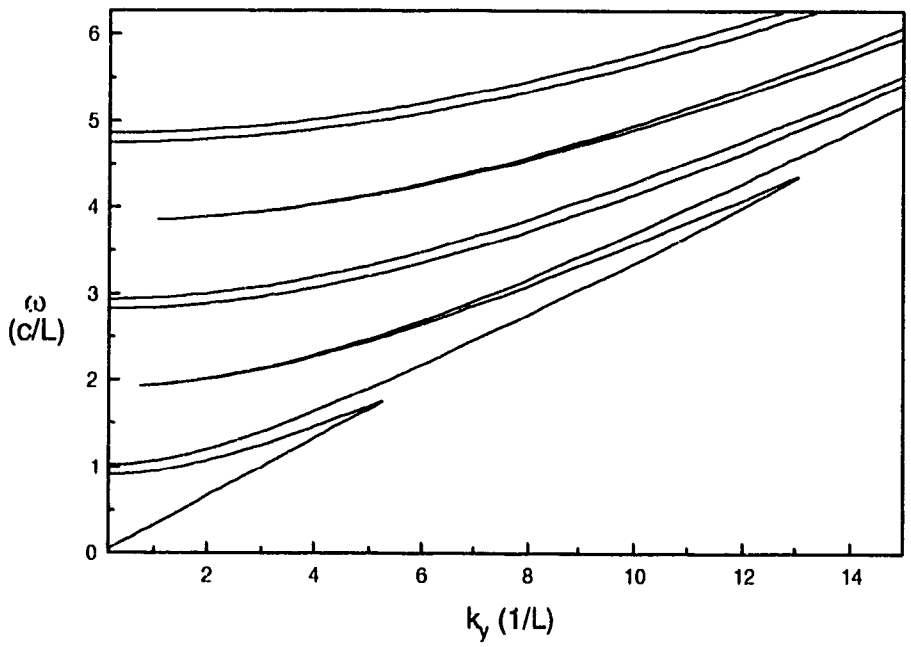

Fig. 2.04. QW stacks, band structure for TE waves. The parameters are L=197.7nm, d_1=0.455L, d_2=0.545L, n_1=3.59, and n_2=3.

Here, k_y=0 corresponds to θ=0, (normal incidence), i.e., k_z=k. The oblique limit corresponds to $\theta=\pi/2$ and any other angle between these two limits would correspond to a straight line passing by (0,0), between the y axis and the oblique limit. At θ=0, a QW structure has only odd gaps but at other angles, even and odd gaps appear.

Fig. 2.05 shows the dispersion relation for TM waves in the same structure. At a certain angle of incidence, there is no gap at all. This can be explained by considering that at each interface, the electromagnetic wave is partially reflected and partially transmitted. When the reflected waves build up (constructive interference), the transmission can be completely inhibited[4], and forbidden bands occur. But for TM waves there is a certain angle, the Brewster angle α_B, defined in terms of the indices of the incidence medium (n) and the transmission medium (n') by

$$\alpha_B = \tan^{-1}\frac{n'}{n}, \qquad 2.42$$

at which there is no reflection, and consequently no gap either. The dotted line in Fig. 2.05 corresponds to the Brewster's angle.

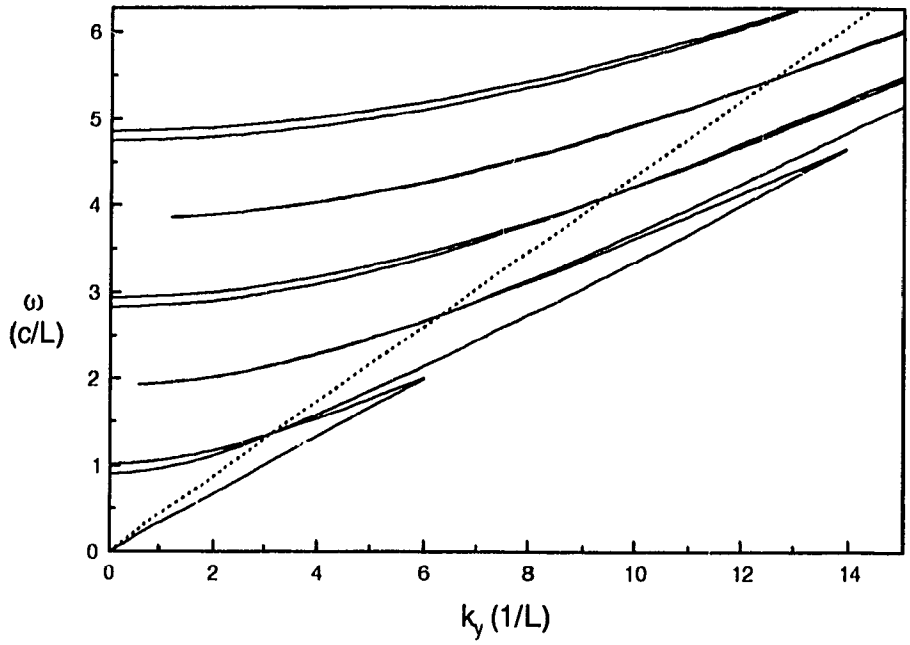

Fig.2.05. QW stacks, TM band structure. The parameters are L=197.7nm, d_1=0.455L, d_2=0.545L, n_1=3.59, and n_2=3.

In the study of the gap variations, we will give results only for θ=0 . Since the gaps for TE and TM waves are similar at this angle of incidence, we will only treat the TE waves.

For non QW two-layered periodic structures, the even gaps exist even at normal incidence as shown in Figs. 2.06 and 2.07. The absence of gap at the Brewster angle is still apparent in Fig. 2.07.

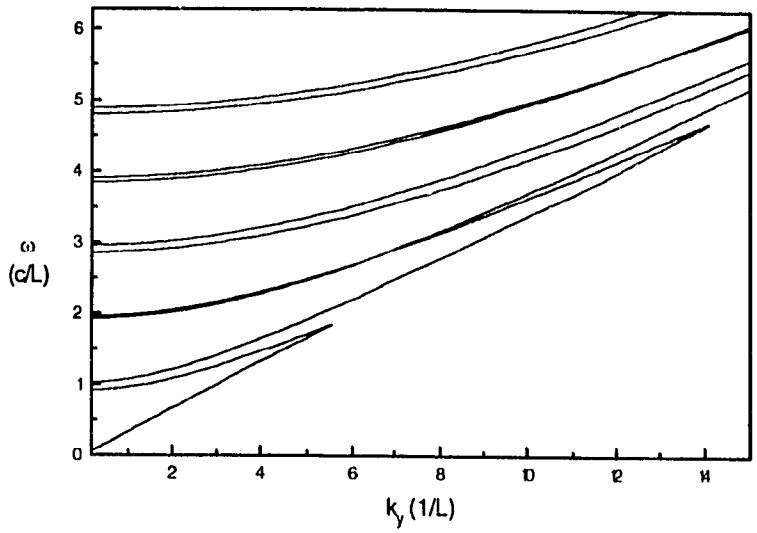

Fig. 2.06. Non QW, band structure for TE waves. The parameters are L=197.7nm, d_1=0.41L, d_2=59L, n_1=3.59, and n_2=3.

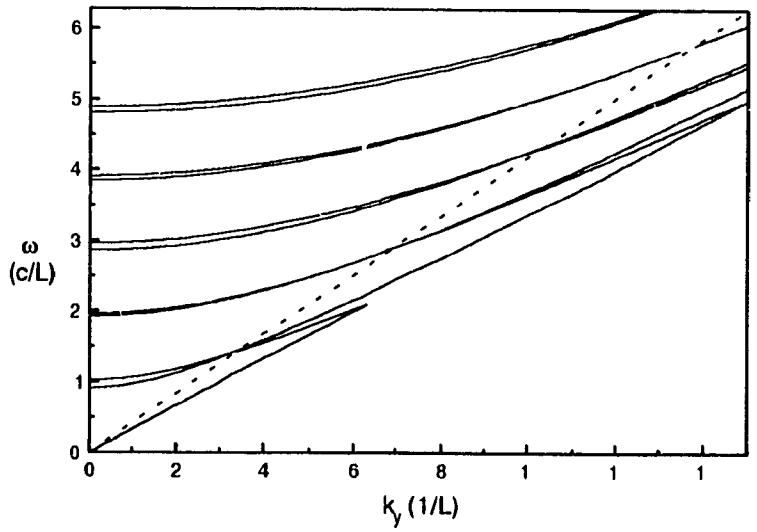

Fig. 2.07. Non QW, TM band structure. The parameters are L=197.7nm, d_1=0.41L, d_2=0.59L, n_1=3.59, and n_2=3.

Let us now see what happens when the width of one layer, say the one with the highest index, varies from zero (no periodic structure) to the whole width of the unit (no periodic structure again). In figure 2.09, we plot graphically the gap width $\Delta\omega$ versus the first layer's width for a normal incidence.

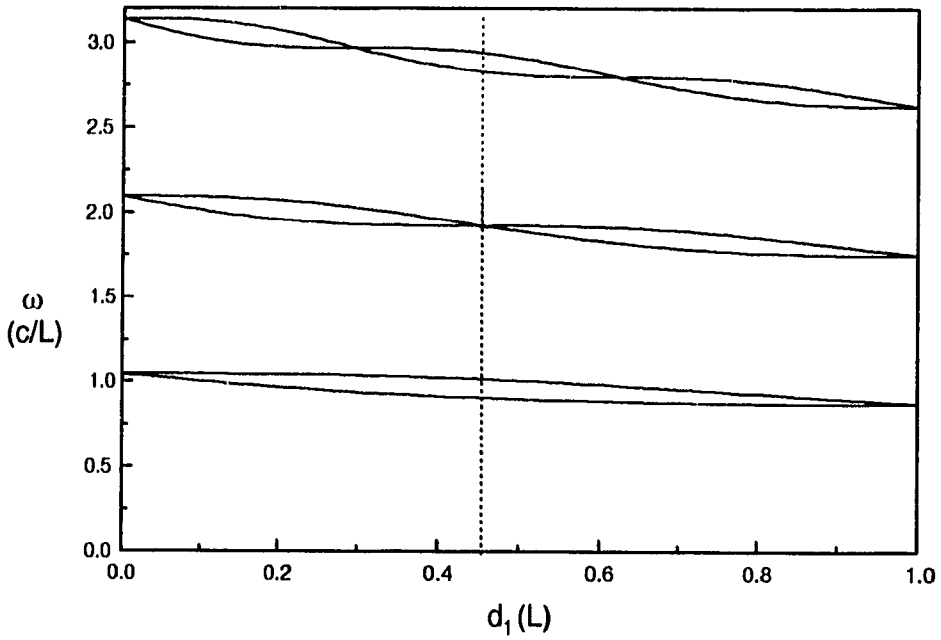

Fig. 2.08 Frequency vs first layer's width. The parameters are L=197.7nm, n_1=3.59, n_2=3, d_2=L-d_1, the dashed line corresponds to a QW stack.

For a QW stack structure (dotted vertical line) we only have the odd gaps as seen before, all equal. Other maxima correspond to constructive interference of different reflected waves which happens when the layers' widths fulfill the condition $(2\alpha+1)d_1n_1=(2\beta+1)d_2n_2$, α,β= 0, 1, 2, 3,..., and $2\alpha d_1n_1=2\beta d_2n_2$ correspond to minima i.e., to zero. Fig. 2.09 shows how gaps change with the first layer's width,

with maxima at d_1=0.145 L, 0.21L, 0.455L(QW), 0.71L and 0.81L. as predicted. For the same unit width, the thiner the layer with the higher refractive index, the larger the maximum gap and the higher the midgap values as Figs 2.07 and 2.08 indicate.

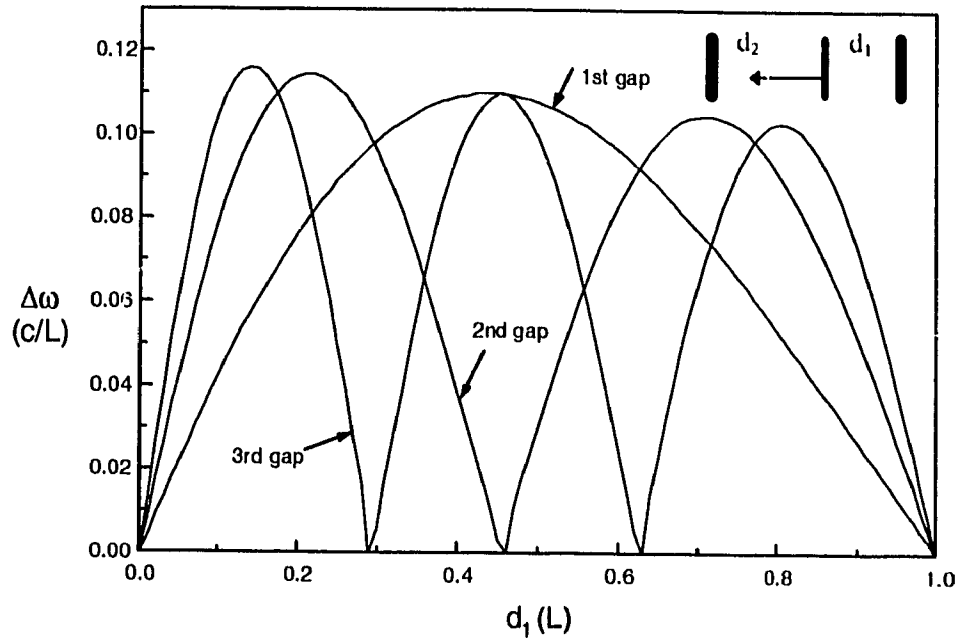

Fig. 2.09. Gaps vs first layer' s width. The parameters are, L=197.7nm, n_1=3.59, n_2=3, d_2=L-d_1 .

If we now consider four layers per unit instead of two, as shown in Figs. 2.10 and 2.11, we obtain a similar result as for a non QW structure, i.e., odd and even gaps and no gap at the Brewster angle . Thus, the results for four-layered units are similar to those for two-layered units. However, there are also some important differences that will be emphasized below.

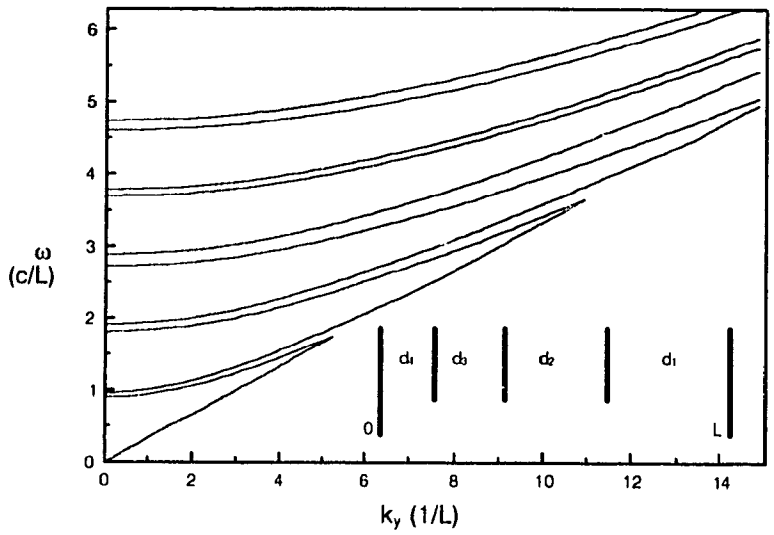

Fig. 2.10. Four-layered units, band structure for TE waves. The parameters are L=197.7nm, d_1=0.455L, d_2=0.272L, d_3=0.163L, d_4=0.11L, n_1=n_3=3.59, and n_2=n_4=3,

Let us now investigate how gaps change as a function of the extra layer's index (n_3 or n_2). As shown in Fig. 2.12, at n_3=3.0 we have a two-layered QW structure, the first gap is at its maximum (odd gap) and the second is equal to zero. These widths will decrease or increase linearly with respect to the index n_3. When n_3 reaches its maximum value, the first band gap drops to 57 % of its original value, whereas the second gap increases up to 93% of the maximum value.

Now, if we consider that the third layer moves inside the unit, the first gap decreases until the extra layer is in the middle of the second layer, see Fig. 2.13. At the same time, the second gap increases and becomes larger by 60% relative

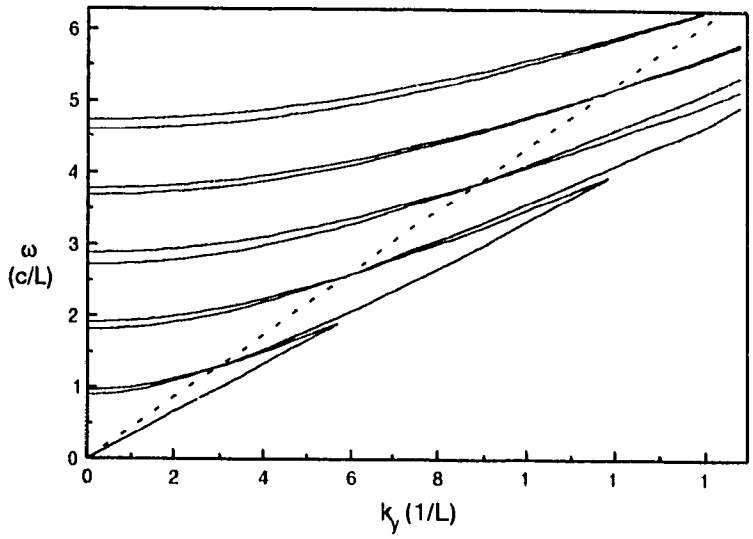

Fig. 2.11. Four-layered units, band structure for TM waves. The parameters are the same as those of Fig. 2.10.

to the QW value. When the third layer is adjacent to the first one, we have only the odd gaps (QW two-layered structure), all equal to $\Delta\omega_{QW}$. The first gap reaches a minimum of 44% of $\Delta\omega_{QW}$ when the second and the fourth layers have the same width.

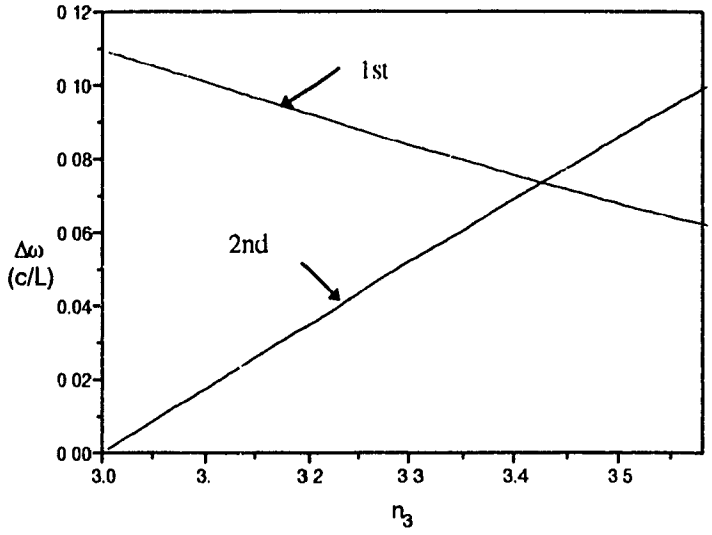

Fig. 2.12. Gaps vs refractive index of the 3rd layer. The parameters are L=197.7nm, d_1=0.455L, d_2=0.272L, d_3=0.163L, d_4=0.11L, n_1=3.59, and n_2=n_4=3.

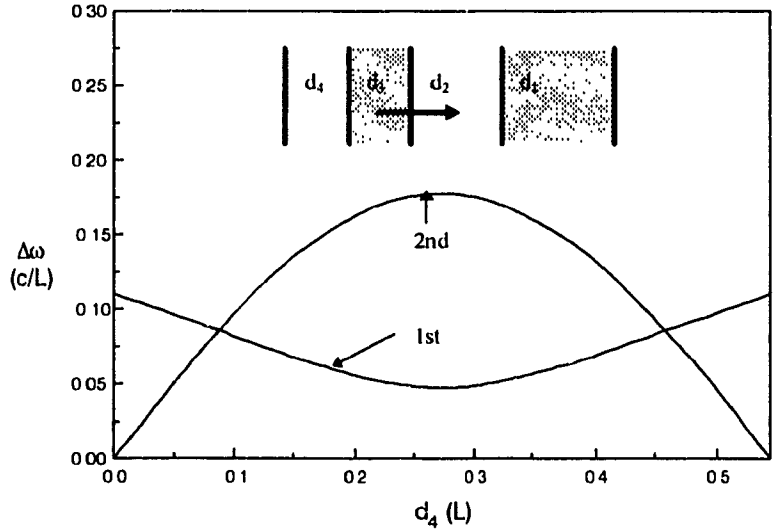

Fig. 2.13. Gaps vs position of the 3rd layer. The parameters are n_1=n_3=3.59, n_2=n_4=3, L=197.7nm, d_1=0.319L, d_3=0.136L, and d_2=0.545L-d_4

When the extra layer is placed in the middle of the second one, the variation of the gaps with the 3rd layer's width is shown in Fig. 2.14.

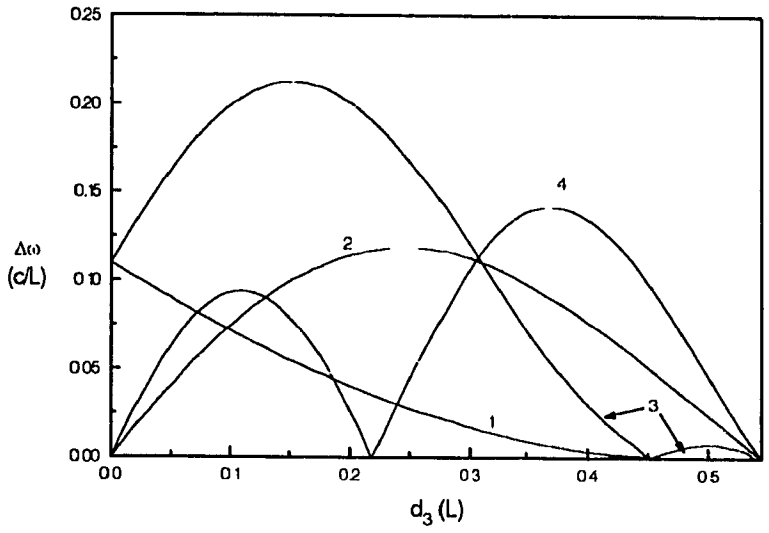

Fig. 2.14 Gaps vs width d_3 of the extra layer. The parameters are L=197.7nm, d_1=0.455L, and d_2=d_4.

At d_3=0, we have a QW structure. In this case, there are only odd gaps. As shown in Fig. 2.14, the first gap decreases uniformly and hits the zero when the third and the first layers have the same width. All odd gaps vanish at this value of d_3. The structure unit can be divided into two units of a non QW periodic structure. The second gap has a maximum a little higher than the QW gaps (8% wider). The third gap reaches twice its starting value before falling down to zero. The fourth gap has two maxima, the first lower by 15% and the second larger by 29% than the QW gap.

A major difference between two-layered and four-layered structures is shown in Figs. 2.09 and 2.14, when we compare the maxima of the third gaps. For the same unit width, the four-layered structure has a maximum gap twice as large as the maximum gap of the two-layered structure.

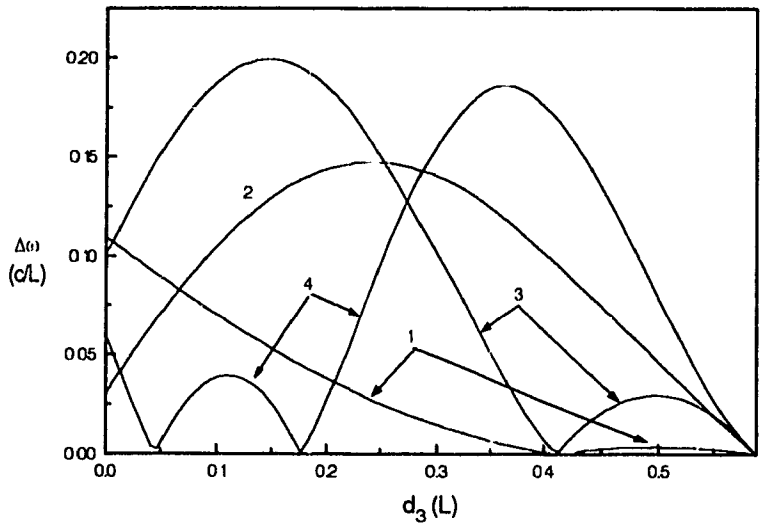

Fig. 2.15 Gaps vs width d_3 of the extra layer (non QW limit). The parameters are L=197.7nm, d_1=0.41L, and d_2=d_4.

If we start with a non QW structure, the second and the fourth gaps do not vanish at d_3=0. For certain values of d_3, they can change by a factor of 4 as shown in Fig. 2.15. Eventually, all gaps vanish when the extra layer takes all the place as the index is uniform along the whole unit.

If the refractive index of the extra layer changes linearly, as shown in Figs. 2.16 and 2.17, the general picture is the same as for four ordinary layers.

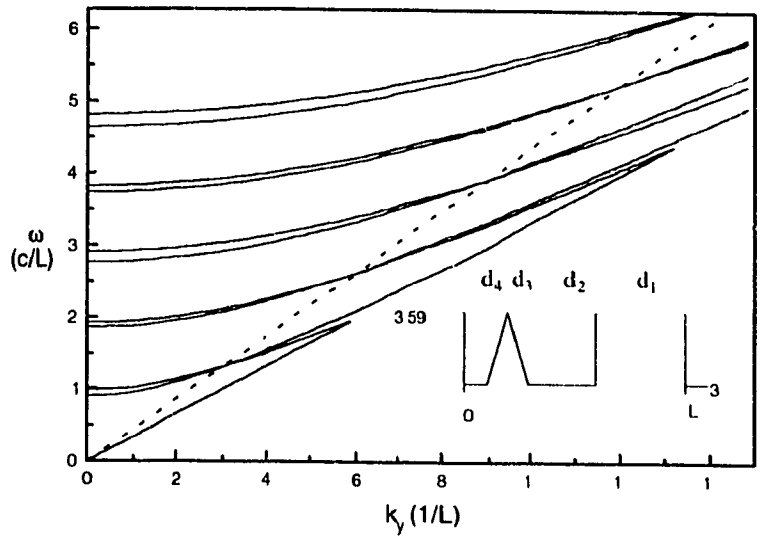

Fig. 2.16. Gradual third layer index change, TM waves. The parameters are L=197.7nm, d_1=0.46L, d_2=0.27L, d_3=0.16L, d_4=0.11L, n_1=3.59 and n_4=3.

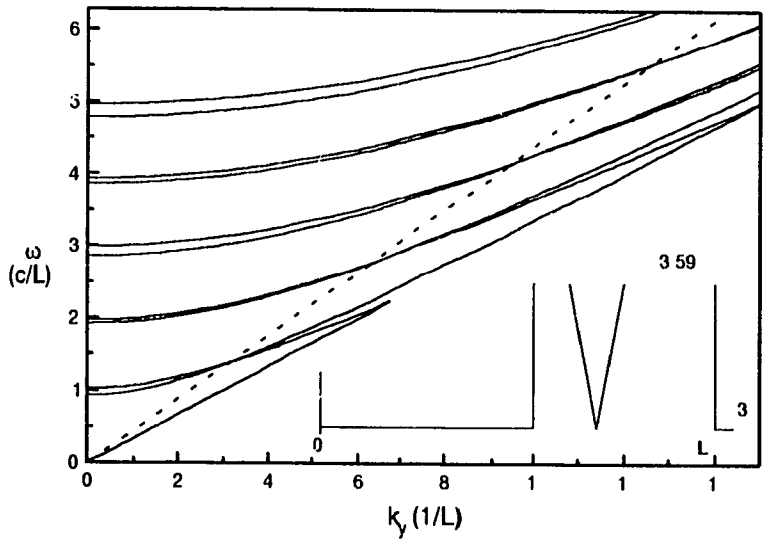

Fig. 2.17. Gradual second layer index change, TM waves. The parameters are L=197.7nm, d_1=0.23L, d_2=0.14L, d_3=0.09L, d_4=0.54L, n_1=3.59 and n_2=3.

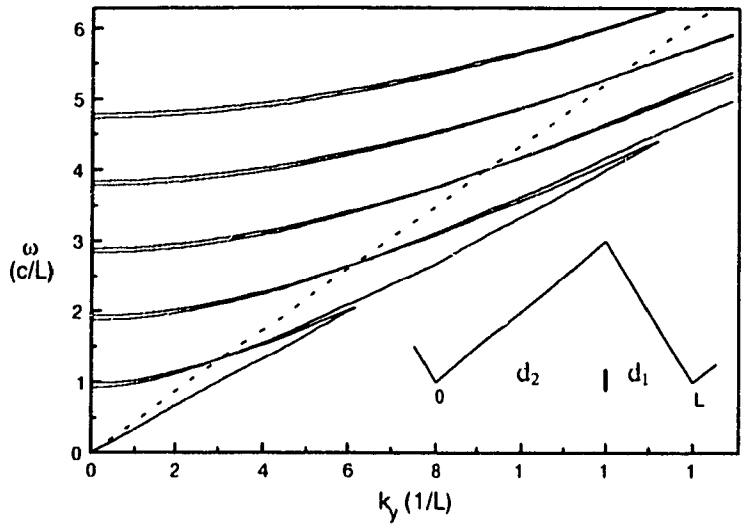

Fig. 2.18. Gradual index throughout the unit, TM waves. The parameters are d_1=90nm, d_2=107.7nm, n_{min}=3, and n_{max}=3.59.

In such a structure, we have a gap pattern similar to that of Fig. 2.11 (similar midgaps) but the second gap is twice smaller than that of its counterpart in Fig. 2.11.

In Fig. 2.18, the index varies linearly throughout the unit; as a result, we have the first gap that is the most noticeable ($\Delta\omega_1/\omega_1$=7.5% for a midgap ω_1 = 0.995); the other gaps are very small ($\Delta\omega_2/\omega_2$ = 0.3% with ω_2=1.99). The result for the first gap is comparable to the results of a QW structure ($\Delta\omega_1/\omega_1$=15 %, ω_1=1). As the Brewster's angle is given by the index contrast between adjacent layers, when the change of index is gradual, those layers have almost the same index and the angle will be equal to 45°.

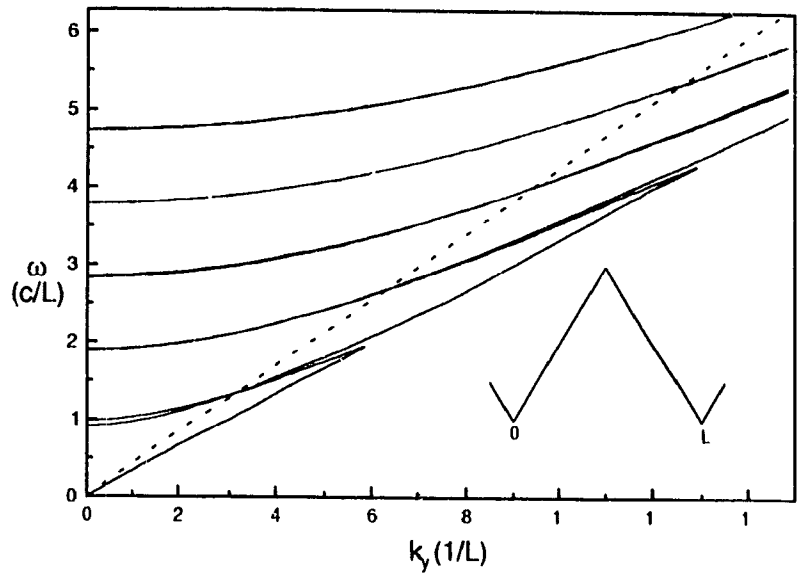

Fig. 2.19. Symmetric gradual index throughout the unit, TM waves. The parameters are n_{min}=3, n_{max}=3.59, and L=197.7nm.

In addition all band gap widths are very close, the deviation for the first three is less than 1%.

A dramatic change occurs when the the index pattern is symmetric as shown in figure 2.19. The relative band widths ($\Delta\omega/\omega$) for the first, second and third gaps are respectively divided by 1.25, 10 and 3 and have absolute values of 0.06, 0.006, and 0.02 c/L.

A well-known phenomenon in optics is the suppression of the reflection of light at the interface between two different media by putting between them a layer of index equal to their geometric mean[4], $n_i = \sqrt{n_1 n_2}$.

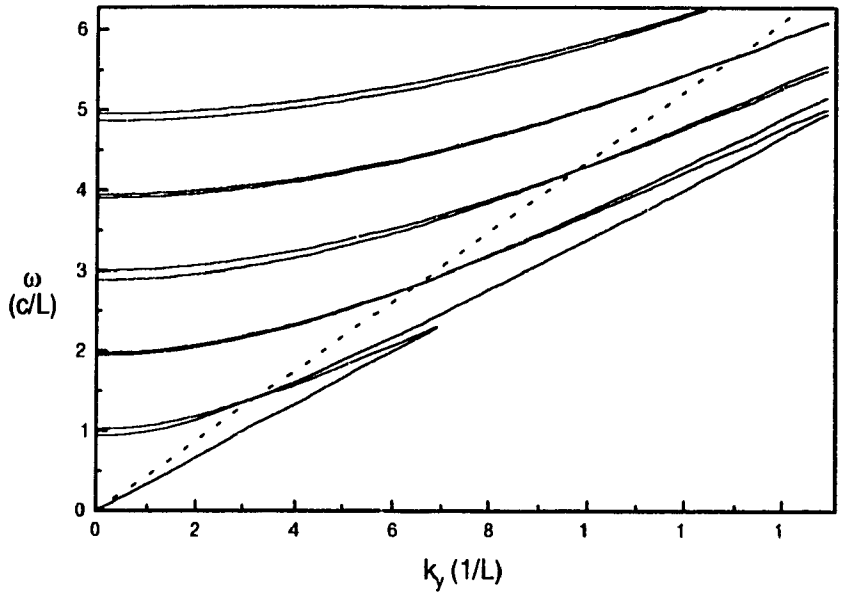

Fig. 2.20. Three-layered units, TM waves. The parameters are L=197.7nm, d_1=0.137L, d_2=0.318L, d_3=0.545L, n_1=3.59, n_2=3.38, and n_3=3.

In general, a three-layered periodic structure has odd and even gaps of different widths as shown in fig. 2.20. The TE case does not have anything special, consequently, we plot only the TM case in order to show the Brewster angles. Here, they ought to be, respectively, equal to 46° and 51.7° for the first and the second inerfaces. Again, they are too close to be distinguished and we show only one corresponding to the dashed line. The values at 0° are the same for TE and TM waves.

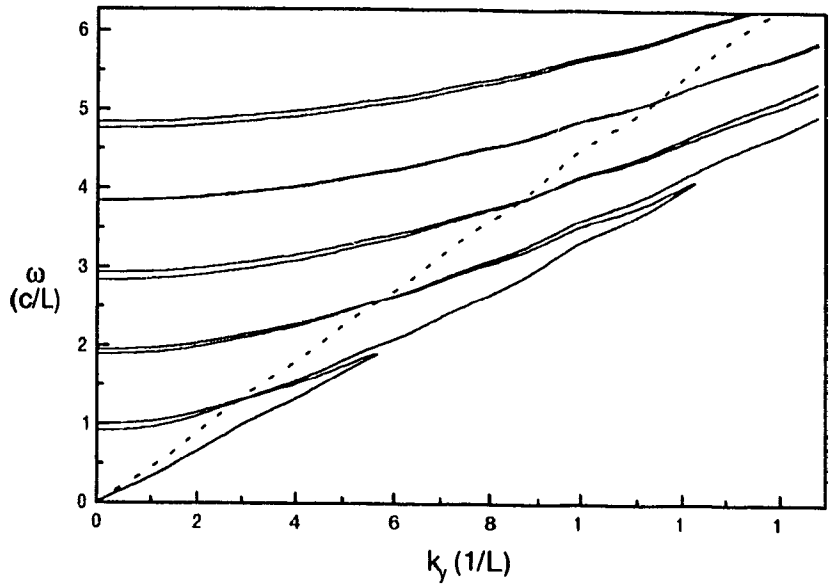

Fig. 2.21. Three-layered units, TM waves, suppressed reflection. The parameters are L=192nm, d_1=0.47L, d_2=d_3=0.265L, n_1=3.59, n_3=3, and $n_2 = \sqrt{n_1 n_1}$.

The gaps are considered as the reflection build-up of all interfaces that interfere constructively until no wave at all is transmited. In a two-layered QW structure, the wave undergoes two reflections, and for an even-multiple frequency of the fundamental, the second reflected wave is π radians out of phase with the first one, and thus interferes destructively, while the third interferes constructively with the first reflection. In total the even gaps will vanish. If now we suppress the second reflection by the addition of a third layer of suitable index, one may expect a band structure where all odd bands would be equal and regularly spaced (at multiples of the fundamental QW frequency) but where even

bands would be still there because the first reflection is no longer there to annihilate them. The results in Fig. 2.21 seem to confirm that at normal incidence.

Gaps at a particular angle of incidence can be derived directly from the dispersion relation (Eq. 2.35). Results are plotted in Fig. 2.22 for a four-layered

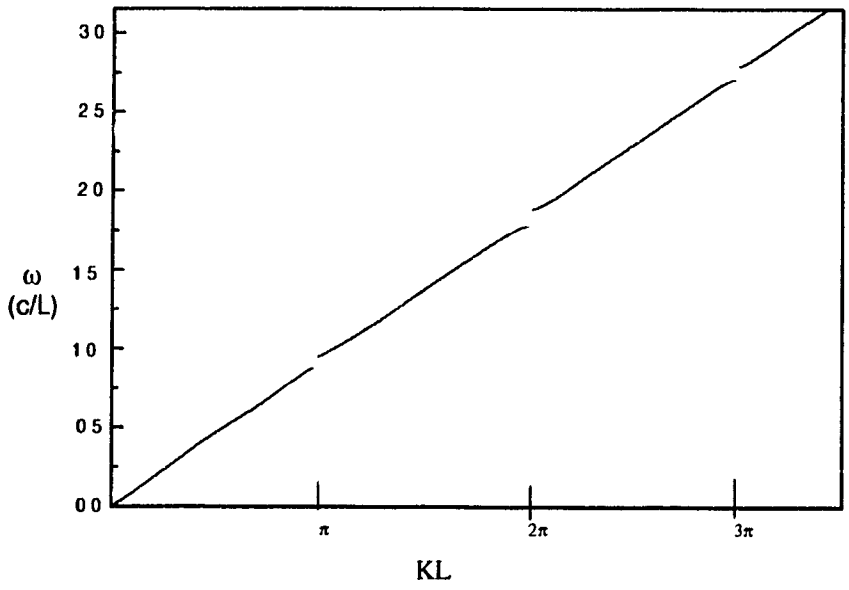

Fig. 2.22. Dispersion relation for a four-layered structure. The parameters are L=197.7nm, d_1=0.455L, d_2= 0.272L, d_3=0.163L, and d_4= 0.11L. The discontinuities at KL=nπ, n=1,2,3 represent the first, second and third photonic gaps, respectively.

infinite structure. When KL is equal to a multiple of π, there is a jump in frequencies, showing the different gaps.

In this chapter, the transfer matrix method has been used to obtain the gaps in multilayered *infinitely* long superlattices as a function of the index and the width of the layers. The next chapter deals with *finite* superlattices.

Chapter 3

FINITE 1D STRUCTURES

3.1 Transmittance of finite periodic structures

In general, the experiments involve finite samples, and very large samples yield results very similar to those of the infinite ones. In infinite structures, we find forbidden bands or gaps for the propagation of electromagnetic waves in the medium. In finite structures, this corresponds to total reflection and the allowed bands are the equivalent of total transmission. In very long samples, the matching is very close, but for small structures, the reflectance is not necessarily equal to one and zero for the forbidden and allowed frequencies, respectively.

The transmittance is generally calculated by taking the nth power of the transfer matrix when we have a finite structure with N identical units, and we compare the amplitude of the incident wave to that of the reflected and transmitted waves[45]. As the transfer matrix is unimodular, its Nth power is given by Eq. 3.01:

$$M^N = \begin{pmatrix} M_{11}U_{N-1} - U_{N-2} & M_{12}U_{N-1} \\ M_{21}U_{N-1} & M_{22}U_{N-1} - U_{N-2} \end{pmatrix}, \qquad 3.01$$

with

$$U_N = \frac{\sin(N-1)KL}{\sin KL} \quad . \qquad 3.02$$

The coefficient of reflection r_N, the reflectance R_N, and the transmittance T_N are defined by Eq. 3.03. According to Eq. 2.31, they can be connected to the transfer matrix by Eq. 3.04:

$$r_N = \left(\frac{B_0}{A_0}\right)_{B_N\,0} \quad , \quad R_N = |r_N|^2 \quad , \quad T_N = 1 - R_N \; ; \qquad 3.03$$

$$r_N = \frac{M_{21}U_{N-1}}{M_{11}U_{N\,1} - U_{N\,2}} \quad . \qquad 3.04$$

An example of the transmittanceof various 5- unit structures as a function of the frequency is shown in Fig. 3.01

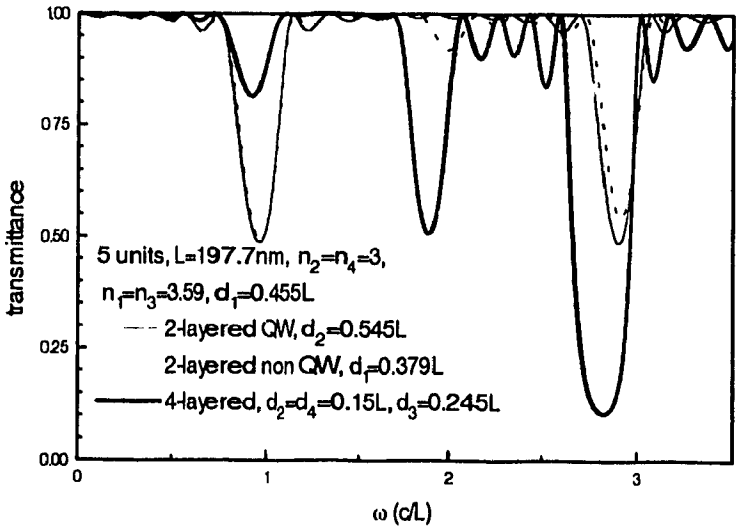

Fig. 3.01. Transmittance for 5-unit structures.

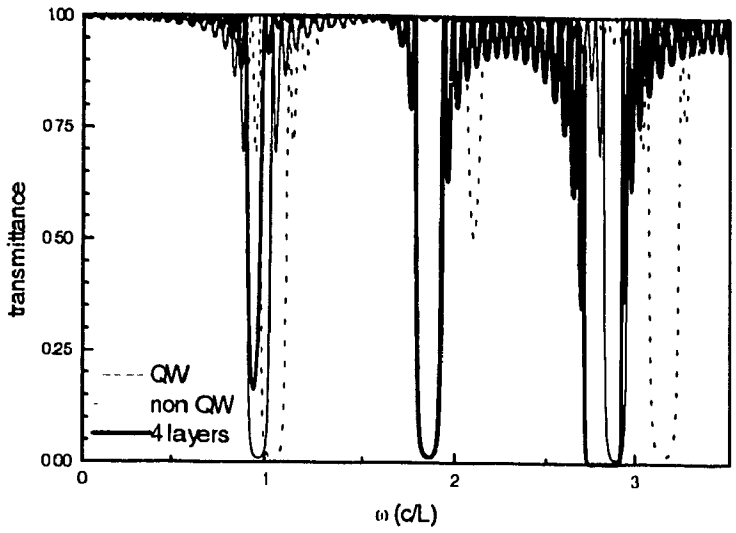

Fig. 3.02. Transmittance for 17-unit finite structures. The labels QW and non QW pertain to two-layered units. The parameters are the same as those of Fig. 3.01.

Let us try to see how the transmittance varies with the number of units for QW, two-layered, and four-layered structures. We expect the transmittance pattern to match more closely the gap profile as the number of units increases.

Figures 3.01 and 3.02 show when the optical path is the same in a two-layered structure (QW case), the minima are equal and placed at odd multiples of the frequency of the first of them. The larger the number of units, the deeper the minima: 0.49 for five units, 0.009 for 17 units and 0 for 50 units.

The insertion of an extra layer in one of the QW layers, in addition to generating another minimum between the odd ones, makes the minima different.

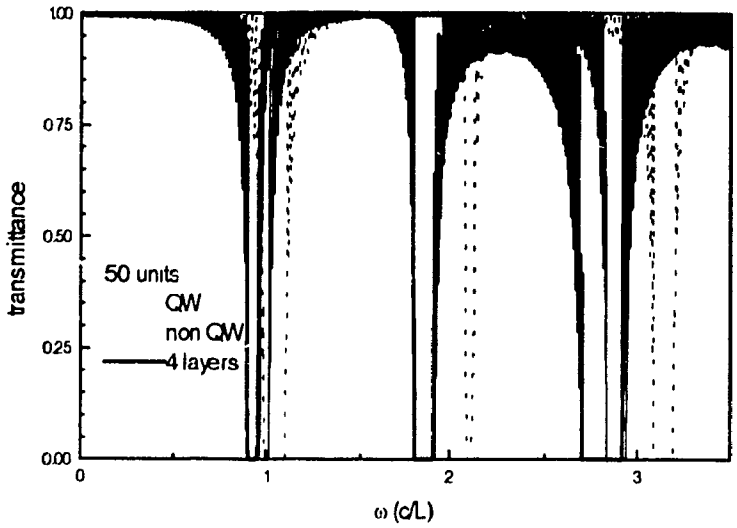

Fig. 3.03. Transmittance for 50-unit structures. The parameters are the sarne as for Fig. 3.01.

The first isolated minimum is higher than the second one which in turn is higher than the third minimum. The latter is 0.10 for 5 units and for 17 units, we have practically no transmittance in a gap 7.3% wide in relative value ($\Delta\omega/\omega$).

For a QW structure, we change only the width of one layer, and we get still another transmittance pattern. As expected from what is known about infinite periodic structures (Fig. 2.05), an extra minimum is inserted between odd minima. The third minimum is deeper than the first, and the second minimum becomes deeper as the number of units increases, dropping from 0.92 for 5 units to 0.51 for 17 units but it is still different from zero even for 50 units.

We can foretell that for more units the transmittance pattern will look like the gap pattern. So, most of the conclusions that were valid for infinite

structures hold approximately for a very large number of units. For a very limited number of units, the lateral fringes are few and shallow; for a large number of units, the lateral fringes are numerous and very thin. It is therefore possible to select desired frequencies with a proper choice of a layered structure or by varying the number of units.

We now consider the case when electromagnetic waves undergo losses while traveling through one absorbing layer. This means that if one refractive index is complex[14], the transmittance will decay exponentially with the frequency and the larger the number of units, the faster the decay. In the results of Fig. 3.04 we have taken a complex index n_2=3.0 - 0.05i. The minus sign in this expression indicates that there is loss of energy in the layer. Even the plot for a four-layered structure with losses follows an exponential decay. The minima do not change compared to the same structure without losses. Near the gap edges, the transmittance drops to 40 % of the incident waves (in energy) for the first gap and as low as 5 % for the second gap of the QW structure. For the 50-unit structure, the transmittance at the edges of the first gap is 3 % and for higher frequencies it drops rapidly to zero.

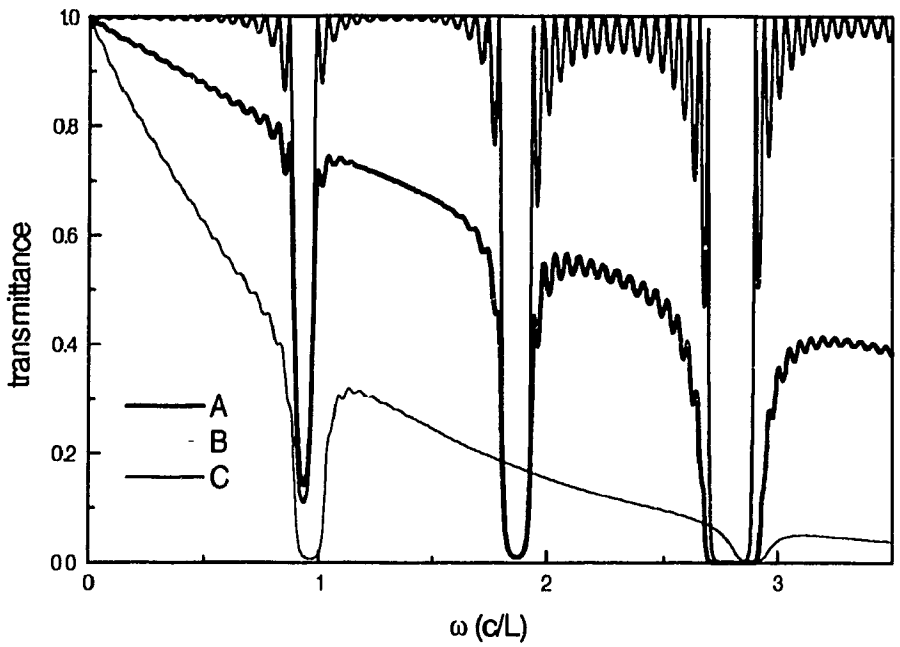

Fig. 3.04. Transmittance for a 17-unit QW structure with losses (C), a 17-unit four-layered structure with losses in one layer (A) and a 17-unit four-layered structure without losses (B). The parameters are the same as those of Fig 3.02, except for the refractive index of the layer with losses.

Considering the case of three layers per unit with one layer acting as anti-reflection medium (see chapter 2), a few units exhibit a transmittance very similar to the one of a QW stack , for which all the minima have the same value (0.49), at odd multiples of the fundamental frequency (Fig. 3.05). For more units, very thin pseudo-gaps appear at even frequency multiples(Fig. 3.06). For 50 units, the transmittance is 0.6 at $\omega=2\omega_0$.

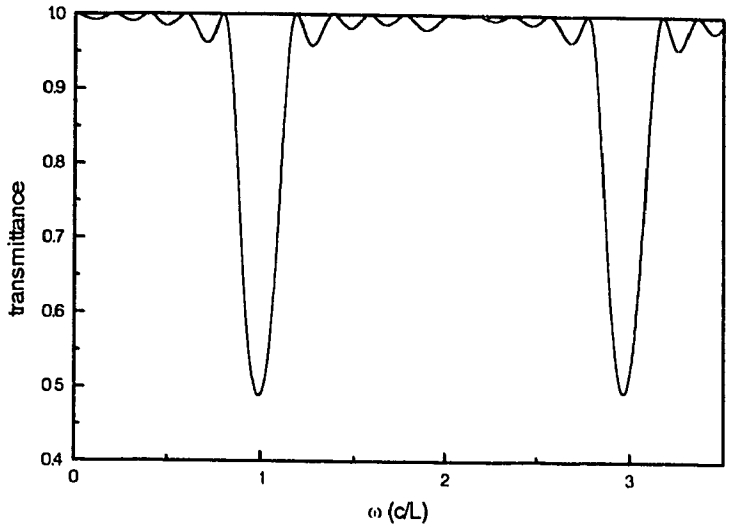

Fig. 3.05. Transmittance with an antireflection layer(5 units). The parameters are L=197.7nm, d_1=0.455L, d_2=d3=0.26L, n_1=3.59, n_2=3.28, and n_3=3.

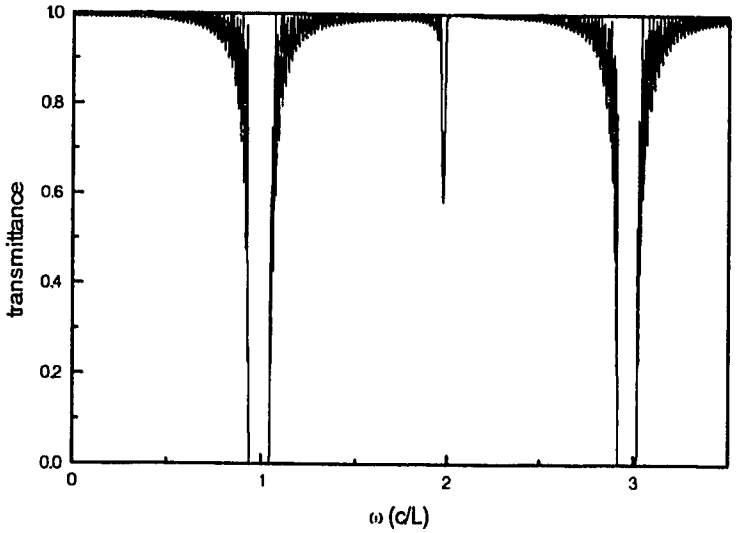

Fig. 3.06 Transmission with an antireflection layer (50 units).

3.2 Pseudoperiodic structures

Sometimes, one wishes to transmit electromagnetic waves concentrated in a very narrow band, or inversely, to reflect only frequencies near a fixed value. Periodic structures with a defect and structures with prearranged succession of layers, such as Fibonacci chains, can meet such conditions. On the other hand, one does not want unpredicted wavelengths to be reflected or transmitted. Hence, one must study the influence of random variation of the layers' widths around some nominal values.

3.2.1 Missing layers

One or more missing layers have as a consequence the introduction of allowed states in the forbidden band, in analogy with donor or acceptor levels in semiconductor electronic bands.

When the 49th layer of a 50-unit bi-layered structure changes its index from n_1 to n_2 (index flipping) , the pseudogap near the left edge of the main gap becomes deeper (see Figs. 3.07 and 3.08) thus isolating a shallow level corresponding to a donor lever in the electronic terminology. The transmittance in this level attains a maximum value M=0.97 for a minimum m=0.02, this represents a change of more than 16 db.

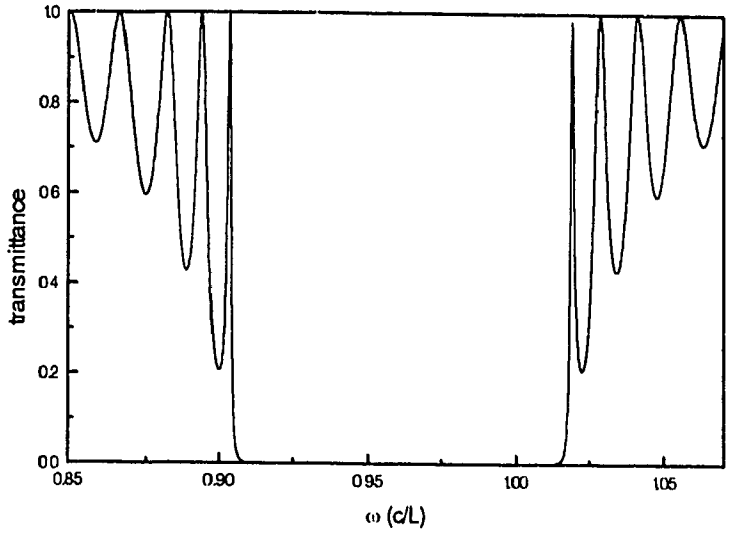

Fig. 3.07. Transmission near the first band gap(50 units). The parameters are L=197.7nm, d_1=0.455L, d_2=0.545L, n_1=3.59, and n_2=3.

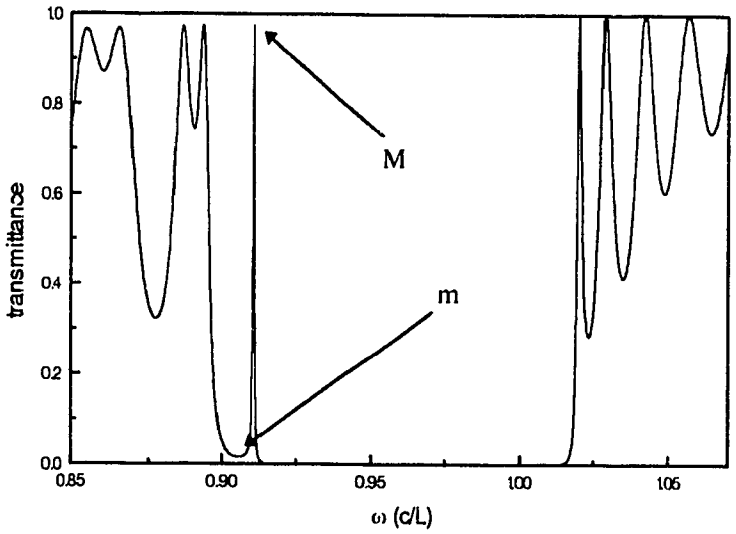

Fig. 3.08. Index flip for the 49th layer. Other parameters are the same as those of Fig. 3.07.

If the index of the 50th layer flips from n_2 to n_1, the level in the gap shifts to the right edge (equivalent to an acceptor in the electronic band theory) but otherwise the transmittance has the same characteristics.

3.2.2 Fibonacci Chains

One of the most studied quasi-periodic arrangements are the Fibonacci chains[17] defined as follows: Suppose we have two different layers, say one long L the other short S. Different Fibonacci chains, made out of these units are given in table 3.01.

F_0	L	
F_1	LS	
F_2	LSL	F_1F_0
F_3	LSLLS	F_2F_1
.....	.....	.....
F_{n+1}	LSLLSLSL.....	F_nF_{n-1}

Table 3.1. Fibonacci chains, L for long, S for short.

These chains are of interest since they are intermediate between the perfect order of periodic systems and systems where n varies randomly. We have already seen that a limited random change introduces new states in an ordered system.

The results for the transmittance of a 34-layered Fibonacci chain[12] shown in Fig. 3.09 can be compared to those of a QW sequence of 17 units in which the first gap is centered at ω=0.961, and has a width $\Delta\omega$=0.112 (see Fig. 3.02). Here we observe two very deep pseudo-gaps centered at ω= 0.73 and ω=1.19 with the same width $\Delta\omega$=0.1.

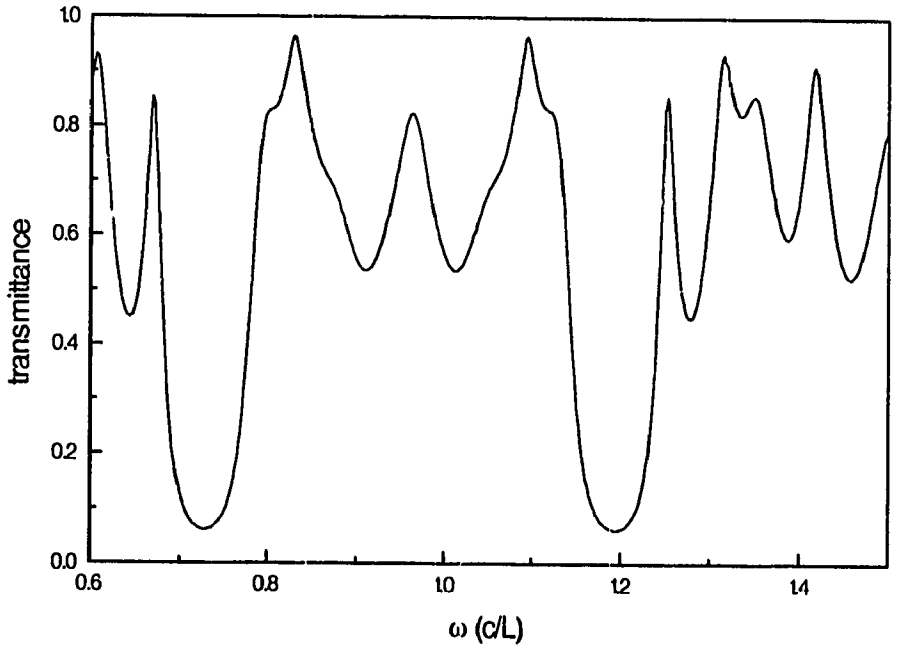

Fig. 3.09. Transmittance for a 34-layer Fibonacci chain. The parameters are 21 layers with d=90nm, n=3.59, and 13 layers with d=107.7nm, n=3, L=197.7nm.

Another interesting feature about the Fibonacci chain is that if we make a Fibonacci sequence of 21 layers of the lowest index and 13 of the highest, we still have the same transmittance profile.

Pseudoperiodic structures like Fibonacci chains are very different from random sequences made of the same layers as Figs. 3.09 and 3.10 show; Jeffries[18] reached a similar conclusion using a Thu-Morse pseudoperiodic arrangement.

Fibonacci chains have been made experimentally[12] and the theoretical gap values were found to closely match the experimental ones.

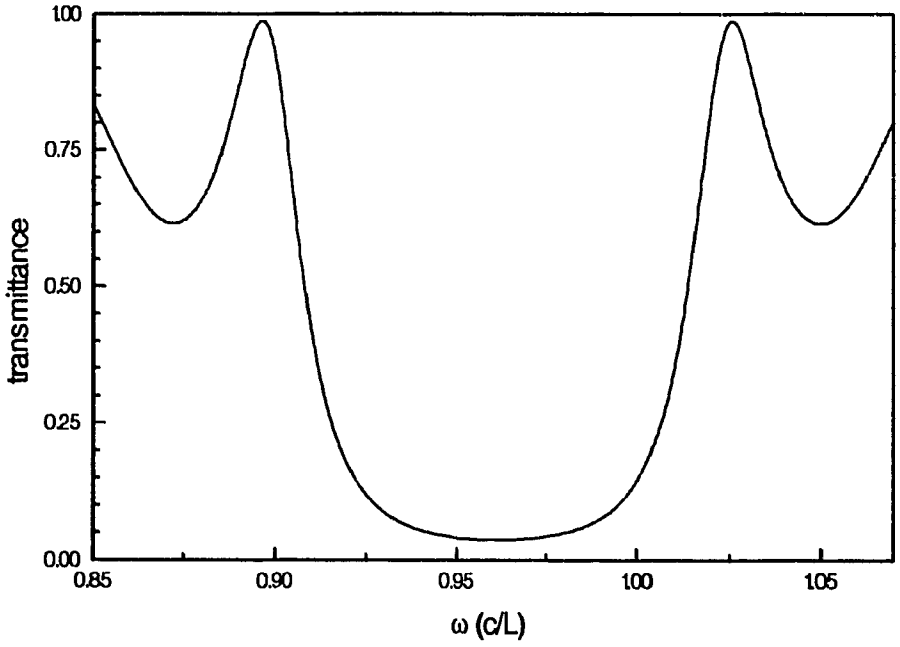

Fig. 3.10. Random sequence of 34 layers. The layers' parameters are the same as those of Fig. 3.09.

In this chapter, finite periodic structures have been studied and structures with 50 units have been found to yield results that are very similar to those of the infinite structures. If only a significant decrease in the transmission is desired, a small number of units can be sufficient. Pseudoperiodic structures, such as Fibonacci chains and periodic sequences with missing layers, help introduce thin allowed levels in the gaps at the desired frequencies. The introduction of an antireflection layer in a unit will introduce narrow pseudo-gaps at even multiples of the fundamental frequency without any noticeable change in the odd values.

With this chapter, we conclude the study of 1D structures. In the next chapter we consider 2D structures.

Chapter 4

2D STRUCTURES

4.1 2D Description

The 2D structures we will be studying have in general the lattice form of Fig. 4.1 below. The rods are infinitely long in the z direction and they have the form of cylinders or prisms with a square cross section. Many authors have worked on similar structures, but all of them were interested in the very existence of the photonic gaps[39, 40, 26, 33], not in their possible modulation. Again, the band gaps will be tuned by changing the dimensions of the rods and their dielectric constants. The lattice is supposed to be infinite, and this enables us to use the plane-wave method. When modified appropriately, the transfer matrix method of chapter 2 can be used for a finite number of lattice elements[34] in order to obtain the transmittance. Actually, the experimental situation one can have is characterized by a finite number of rods of finite length[33]. However, in what follows we will consider only infinite lattices.

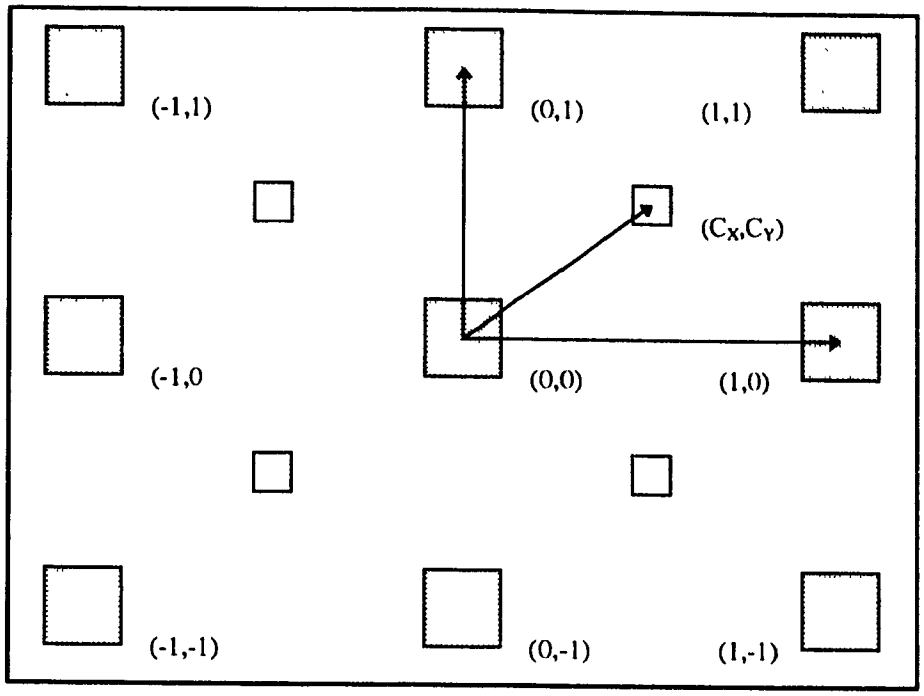

Fig. 4.01. Square lattice of square rods with interstitial rods

4.2. Plane-wave method

The plane wave method consists of considering reciprocal lattice vectors as corresponding to plane waves that constitute a complete basis in which any other wave can be expanded. This method is quite heavily used in electronic band gaps studies in three dimensions[3], in photonic gaps in three[36], two[26], and one[45] dimensions. In the later, it yields the same results as the transfer matrix method.

As the structures are periodic, Fourier analysis is helpful in finding those basis waves. We start again with the wave equations. 2.02 and 2.03 and as-

sume an exponential time dependence of the electric and magnetic fields; that is, we write

$$\vec{X}(\vec{r},t) = \vec{X}(\vec{r})e^{-i\omega t}, \tag{4.01}$$

where $\vec{X} = \vec{E}$ or $\vec{H}$. Inserting this expression in the wave equations,we obtain

$$\begin{aligned} &\nabla\times\nabla\times\vec{E} - \frac{\varepsilon\omega^2}{c^2}\vec{E} = 0, \\ &\nabla\times\left(\frac{1}{\varepsilon}\nabla\times\vec{H}\right) - \frac{\omega^2}{c^2}\vec{H} = 0. \end{aligned} \tag{4.02}$$

In a periodic medium, the eigenfunctions of Eqs 4.02 are given by the Bloch functions[36] $\vec{X}(\vec{r}) = e^{i\vec{k}\cdot\vec{r}}\vec{X}_k(\vec{r})$, where $\vec{X}_k(\vec{r})$ is a function with the periodicity of the lattice. Expanding $\vec{X}_k(\vec{r})$ in Fourier series over the reciprocal lattice vectors $\vec{G}$, we have

$$\begin{aligned} \vec{E}_{nk}(\vec{r},t) &= \vec{E}_{nk}(\vec{r})e^{-i\omega_{nk}t} = e^{i(\vec{k}\cdot\vec{r}-\omega_{nk}t)}\sum_{\vec{G}}\vec{E}_{nk}(\vec{G})e^{i\vec{G}\cdot\vec{r}}, \\ \vec{H}_{nk}(\vec{r},t) &= \vec{H}_{nk}(\vec{r})e^{-i\omega_{nk}t} = e^{i(\vec{k}\cdot\vec{r}-\omega_{nk}t)}\sum_{\vec{G}}\vec{H}_{nk}(\vec{G})e^{i\vec{G}\cdot\vec{r}}. \end{aligned} \tag{4.03}$$

The Fourier coefficients $\vec{E}_{\vec{G}} = \vec{E}(\vec{G})$ and $\vec{H}_{\vec{G}} = \vec{H}(\vec{G})$ satisfy the following equations;

$$\begin{aligned} &(\vec{k}+\vec{G})\times(\vec{k}+\vec{G})\times\vec{E}_{\vec{G}} + \frac{\omega^2}{c^2}\sum_{\vec{G}'}\varepsilon_{\vec{G}\vec{G}'}\vec{E}_{\vec{G}'} = 0, \\ &\sum_{\vec{G}'}\eta_{\vec{G}\vec{G}'}(\vec{k}+\vec{G})\times(\vec{k}+\vec{G}')\times\vec{H}_{\vec{G}'} + \frac{\omega^2}{c^2}\vec{H}_{\vec{G}} = 0; \end{aligned} \tag{4.04}$$

where $\eta(\vec{r}) = 1/\varepsilon(\vec{r})$; the periodicity of the dielectric constant implies

$$\varepsilon(\vec{r}) = \varepsilon_a + \varepsilon_o(\vec{r}-\vec{R}), \tag{4.05}$$

with $\vec{R}$ being a lattice vector.

Now the dielectric constant can be expanded in a Fourier series in reciprocal space and it reads

$$\varepsilon(\vec{G}) = \frac{1}{V_{WS}} \int_{WS} e^{i\vec{G}.\vec{r}} \varepsilon(\vec{r}) d\vec{r}. \qquad 4.06$$

WS stands for Wigner -Seitz cell. Combining Eqs. 4.05 and 4.06 yields

$$\varepsilon(\vec{G}) = \varepsilon_a \delta_{\vec{G}O} + \frac{1}{V_{WS}} \int_{WS} e^{i\vec{G}.\vec{r}} \varepsilon_o(\vec{r}) d\vec{r}, \qquad 4.07$$

where $\varepsilon_o(\vec{r})$ is the dielectric constant measured from ε_a taken as the value of the background. In order to use Eq. 4.04, we have to find the coefficients $\varepsilon_{\vec{G}}$; this can be done by expanding ε_o in a Fourier series.

The main structures we will be dealing with involve cylinders spheres, and prisms. The unit step function will be used to distinguish the regions of different dielectric constants since we will assume an abrupt change of the latter. For spheres we have[36]

$$\varepsilon_0(\vec{r}) = (\varepsilon_a - \varepsilon_b)\theta(R - |\vec{r}|), \qquad 4.08$$

and for cylinders,

$$\varepsilon_o(\vec{r}) = (\varepsilon_b - \varepsilon_a)\theta(R_b - \rho_{xy}) + (\varepsilon_c - \varepsilon_a)\theta\left(R_c - \sqrt{(c_x - x)^2 + (c_y - y)^2}\right). \qquad 4.09$$

We recall[11] that for $\rho_{xy}=\sqrt{x^2+y^2}$, the unit step function θ is defined as

$$\theta(R_b - \rho_{xy}) = cyl\left(\frac{\rho_{xy}}{2R_b}\right) = \begin{cases} 1 \text{ for } \rho_{xy} < R_b, \\ 0 \text{ for } \rho_{xy} > R_b, \\ 1/2 \text{ for } \rho_{xy} = R_b. \end{cases} \qquad 4.10$$

In the case above we will consider two sorts of cylinders in the unit cell: one centered at the origin of the lattice, and another at a point $c_x \vec{i} + c_y \vec{j}$. Their indices and radii are, respectively, ε_b ,R_b, and ε_c, R_c.

Similarly, for prisms with rectangular cross section, we have

$$\varepsilon_o(\vec{r}) = (\varepsilon_b - \varepsilon_a)\,\theta\left(\frac{A_{bx}}{2} - |x|\right)\theta\left(\frac{A_{by}}{2} - |y|\right) + (\varepsilon_c - \varepsilon_a)\,\theta\left(\frac{A_{cx}}{2} - |c_x - x|\right)\theta\left(\frac{A_{cy}}{2} - |c_y - y|\right). \qquad 4.11$$

The refractive index enters the formalism through $(k_o n)^2 = \omega^2\varepsilon/c^2$, where k_o stands for the wave number in vacuum.

For a unit square of side d, Eq. 4.07 yields[51, 52]

$$\varepsilon_o = \theta(d - |x|), \qquad \varepsilon(\alpha) = \frac{2\sin b\alpha}{d\alpha}, \qquad 4.12$$

$$\varepsilon(x,y) = \theta(c - \rho_{xy}) \Leftrightarrow \varepsilon(G_{xy}) = \frac{2\pi c J_1(G_{xy}c)}{d^2 G_{xy}}, \qquad 4.13$$

$$\varepsilon(x + a) \Leftrightarrow e^{ia\alpha}\varepsilon(\alpha), \qquad 4.14$$

with

$$\theta(b - |x - c|) \Leftrightarrow e^{ic\alpha}\frac{2\sin b\alpha}{d\alpha}. \qquad 4.15$$

For the prisms with a square cross section of side A_b, the Fourier series coefficients read

$$\varepsilon_o(\vec{G}) = \frac{4(\varepsilon_b - \varepsilon_a)}{d^2} \frac{\sin(A_b G_x/2)}{G_x} \frac{\sin(A_b G_y/2)}{G_y} + \frac{4(\varepsilon_c - \varepsilon_a)}{d^2} e^{-i(C_x G_x + C_y G_y)} \frac{\sin(A_c G_x/2)}{G_x} \frac{\sin(A_c G_y/2)}{G_y}. \quad 4.16$$

For structures with cylinders, ε_o is given by

$$\varepsilon_o(\vec{G}) = \frac{2\pi R_b(\varepsilon_b - \varepsilon_a)}{d^2} \frac{J_1(R_b G_{xy})}{G_{xy}} + \frac{2\pi R_c(\varepsilon_c - \varepsilon_a)}{d^2} e^{-i(C_x G_x + C_y G_y)} \frac{J_1(R_c G_{xy})}{G_{xy}}. \quad 4.17$$

For $\vec{G}$=0, Eqs. 4.16 and 4.18 take the simpler forms

$$\lim_{\vec{G} \to 0} \varepsilon_o = \frac{(\varepsilon_b - \varepsilon_a)}{d^2} A_b^2 + \frac{(\varepsilon_c - \varepsilon_a)}{d^2} A_c^2 \quad , \quad 4.18$$

and

$$\lim_{\vec{G} \to 0} \varepsilon_o(\vec{G}) = \frac{\pi R_b^2(\varepsilon_b - \varepsilon_a)}{d^2} + \frac{\pi R_c^2(\varepsilon_c - \varepsilon_a)}{d^2} \quad , \quad 4.19$$

respectively. The formulae for $\eta(\vec{G})$ are obtained from those for $\varepsilon(G)$ by replacing $\varepsilon_{a,b}$ with $\eta_{a,b}$.

The wave vector $\vec{k}$ varies in the reciprocal space as indicated in Fig.4.02.

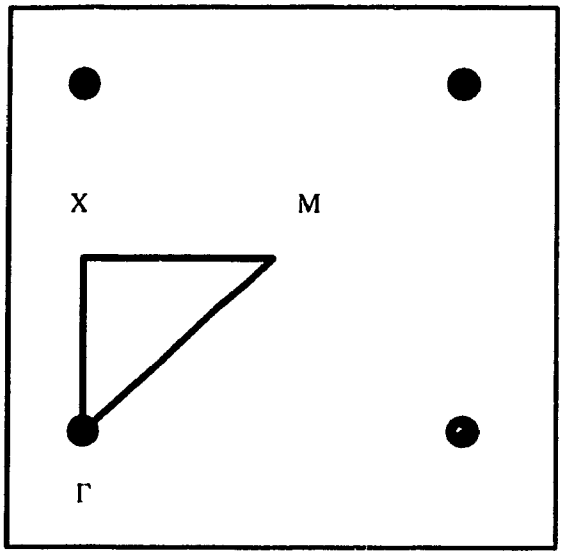

Fig. 4.02. Variation of $\vec{k}$ in the reciprocal space.

To simplify the calculations, we consider the case where the electric field (or the magnetic field) is parallel to the z axis and the dielectric constant varies only along the x and y directions. This means that $(\vec{k}+\vec{G})$is normal to $\vec{E}_{\dot{G}}$ or to $\vec{H}_{\dot{G}}$, that is,

$$(\vec{k}+\vec{G})\perp\vec{E}_{\dot{G}}, (\vec{k}+\vec{G})\perp\vec{H}_{\dot{G}}\,. \qquad 4.20$$

Consequently,

$$\begin{aligned}(\vec{k}+\vec{G})\times(\vec{k}+\vec{G})\times\vec{E}_{\dot{G}} &= -|\vec{k}+\vec{G}|^2\vec{E}_{\dot{G}}\,,\\ (\vec{k}+\vec{G})\times(\vec{k}+\vec{G}')\times\vec{H}_{\dot{G}'} &= -|(\vec{k}+\vec{G})*(k+\vec{G}')|\vec{H}_{\dot{G}'}\,.\end{aligned} \qquad 4.21$$

The reciprocal lattice vectors are given by [3]

$$\vec{G}_{pq} = \frac{2\pi}{g_x}p\vec{i} + \frac{2\pi}{g_y}q\vec{j};\quad p,q = 0, 1, 2, \cdots, \qquad 4.22$$

where g_x and g_y are basis vectors in real space. Equations 4.04 can be written in a matrix form after introducing the following notations:

$$\Theta_{\lambda\lambda} = -\eta(0)\left|\vec{k}+\vec{G}_{ij}\right|^2 + \frac{\omega^2}{c^2},$$
$$\Theta_{\mu\nu} = -\eta\left(\vec{G}_{ij}-\vec{G}_{kl}\right)\left|\left(\vec{k}+\vec{G}_{ij}\right)*\left(\vec{k}+\vec{G}_{kl}\right)\right|, \qquad 4.23$$

and

$$\Omega_{\lambda\lambda} = \frac{\omega^2}{C^2}\varepsilon(0) - \left|\vec{k}+\vec{G}_{ij}\right|^2,$$

$$\Omega_{\mu\nu} = \frac{\omega^2}{C^2}\varepsilon\left(\vec{G}_{ij}-\vec{G}_{kl}\right), \quad \mu\leftrightarrow(kl), \nu\leftrightarrow(ij) \quad \text{for} \quad \mu\neq\nu, \qquad 4.24$$

where $\lambda \in \Lambda = \left\{1,\cdots,(2l-1)^2\right\}$, and $(i,j)\in\Sigma$, $i,j = -\frac{l}{2},-\frac{l}{2}+1,\cdots,\frac{l}{2}$.

There is a bijection between the sets Λ and I, that will link the quantities $\Theta_{\lambda\mu}$ and $\Omega_{\lambda\mu}$ to vectors G_{ij}. Now, Eqs. 4.04 read

$$\begin{pmatrix} \Omega_{11} & \Omega_{12} & \Omega_{13} & \cdots \\ \Omega_{21} & \Omega_{22} & \Omega_{23} & \cdots \\ \Omega_{31} & \Omega_{32} & \Omega_{33} & \cdots \\ \cdots & \cdots & \cdots & \cdots \end{pmatrix}\begin{pmatrix} E_1 \\ E_2 \\ E_3 \\ \cdots \end{pmatrix} = 0, \qquad 4.25$$

and

$$\begin{pmatrix} \Theta_{11} & \Theta_{12} & \Theta_{13} & \cdots \\ \Theta_{21} & \Theta_{22} & \Theta_{23} & \cdots \\ \Theta_{31} & \Theta_{32} & \Theta_{33} & \cdots \\ \cdots & \cdots & \cdots & \cdots \end{pmatrix}\begin{pmatrix} H_1 \\ H_2 \\ H_3 \\ \cdots \end{pmatrix} = 0. \qquad 4.26$$

For a 2D square lattice, we have $g_x=g_y=g$ and some expressions can be simplified:

$$\vec{k} = \begin{cases} s\vec{i} \quad \text{along} \quad \Gamma X, \quad 0 \le s \le \frac{g}{2}; \\ \frac{g}{2}\vec{i} + s\vec{j} \quad \text{along} \quad XM, \\ s\vec{i} + s\vec{j} \quad \text{along} \quad M\Gamma; \end{cases} \qquad 4.27$$

$$k = \frac{n\omega}{c}\cos\varphi; \quad \begin{cases} \varphi = 0 \quad \text{along} \quad \Gamma X, \\ \varphi = \frac{\pi}{2} \quad \text{along} \quad XM, \\ \varphi = \tan^{-1}\frac{Gb}{Ga} \quad \text{along} \quad M\Gamma. \end{cases} \qquad 4.28$$

Equations 4.16 and 4.17 show that the $\Omega_{\mu\nu}$ and $\Theta_{\mu\nu}$ matrices are hermitian for lossless media. Equations. 4.04 can be solved only for those values of ω for which

$$\det(\Omega_{\mu\nu}) = 0, \text{ and } \det(\Theta_{\mu\nu})=0 . \qquad 4.29$$

Only for these cases do non-evanescent electromagnetic waves exist in the periodic structure. If the determinants were not equal to zero, every coefficient E or H would have to vanish in order to satisfy Eqs. 4.29 because the rows of matrices $(\Theta_{\mu\nu})$ and $(\Omega_{\mu\nu})$ would be independent.

For each k, we will find values of ω for which the determinant is zero. Only the projection of the k vector on the xy plane is considered in our case. The relation between k and ω is given by

$$|\vec{k}| = \frac{n\omega}{c}\cos\theta, \qquad 4.30$$

where θ is the angle between $\vec{k}$ and the xy plane.

In order to solve our eigenvalue problem, we have to consider a infinite number of elements. Fortunately, the Fourier coefficients of ε go rapidly to zero when the reciprocal vector increases as Eqs. 4.16 and 4.17 contain sin(x)/x and $J_1(x)/x$, x increasing with the lattice vectors. This is an indication that as we consider more and more elements in reciprocal space, the series converges.

The appearance of sin(x)/x and $J_1(x)/x$ in Eqs. 4.16 and 4.17 indicates that the most important parameter P that determines the gaps is given by

$$P_c = (\varepsilon_b - \varepsilon_a)\frac{\pi R_b^{\,2}}{d^2}, \qquad 4.31$$

for circular cross sections, and

$$P_s = (\varepsilon_b - \varepsilon_a)\frac{A_b^2}{d^2}, \qquad 4.32$$

for square cross sections. In other words, the most relevant quantities are the filling fraction, A_b^2/d^2 and the dielectric constant contrast, ε_b-ε_a. Some authors[63] have already studied the effect of the filling fraction and the dielectric constant contrast on the total gap, i.e., the band width where TM and TE gaps overlap. They do not seem to have any limitation on the dielectric constant and the values they used are generally very high. In the following section we will principally see how the TE gaps vary with values accessible to experiments.

4.3 Numerical results

Most of the 2D structures that have been studied consist of a styrofoam (ε=1.04) background[33, 26], with alumina composite rods (ε=9) at square or hexagonal[40] lattice vectors. Gaps were found theoretically[15, 39, 40] and experimentally[30, 26], and even localized levels were introduced in the gaps[35] by removing some rods. In this section we will investigate how the gaps can be modified by changing the unit of the structures.

As dielectric constants are fixed by the choice of materials, all we are free to change is the dimensions and the position of the rods. We can modify the magnitude of the the lattice basis vectors, by putting intersticial rods in the unit cell or by removing rods. In analogy with the 1D case, we expect to have a

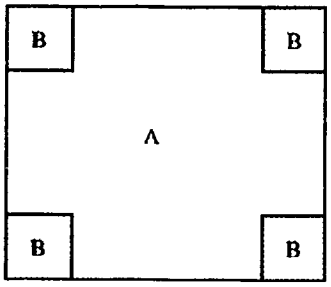

Fig. 4.03. Possible dielectric contrast. The equivalent of a 1D QW is obtained when the condition $(\text{A area})*\varepsilon_A = (\text{B area})*\varepsilon_B$ is satisfied.

maximum gap if we have a 2D equivalent of a QW structure, that is , if the rod-to-styrofoam cross section ratio (the filling fraction) is equal to the inverse of the index ratio (with $\varepsilon \propto n^2$). This is shown schematically in Fig. 4.03.

This is true only for TE waves (s polarisation), and when the dielectric constant of the background is lower than that of the rods. This applies to the results shown in Figs. 4.04, 4.05 and 4.12. As shown in Fig. 4.05, square rods arranged in a square lattice yield a maximum relative bandgap width of more than 30% ($\Delta\omega_1/\omega_1$) for the s polarization but no gap appear for the TM polarization in the

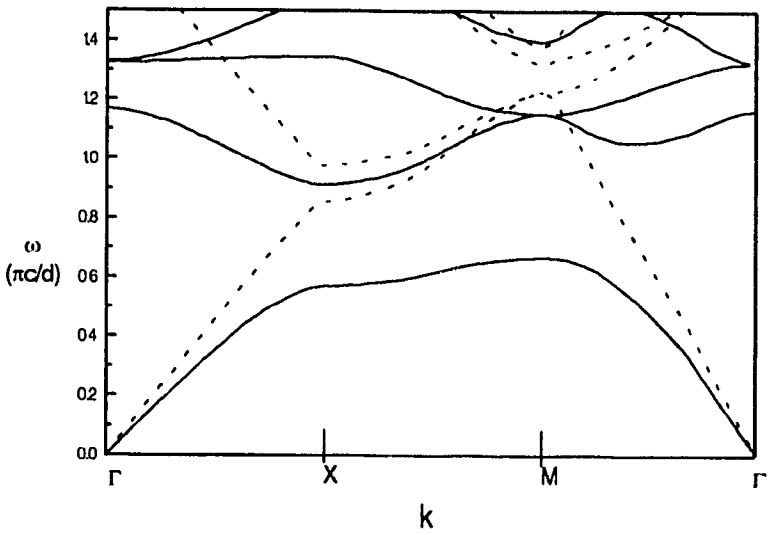

Fig. 4.04. 2D "QW" square lattice with square cross section rods, for TE(solid curves) and TM (dotted curves) waves. The parameters are d=1.27cm, s_b=0.40cm, ε_a=1, and ε_b=9.

same frequency range. Consequently, we give results only for the s polarization as many authors[36, 26, 35] do. All square lattices have d=1.27 cm as the lattice unit vector, s_α is the side of the square cross section rods.

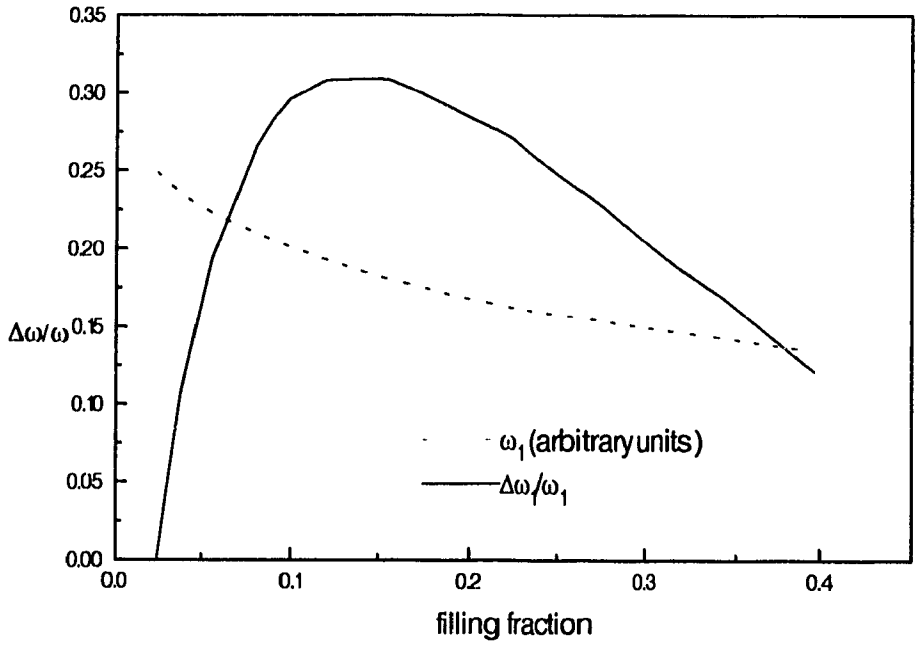

Fig. 4.05. Ratio of the first gap ($\Delta\omega_1$) to the midgap frequency (ω_1) as a function of the filling fraction of square rods of permittivity 9 in a background of permittivity 1.

For ratios other than those of Fig. 4.04, the gaps decrease in importance as shown for example in Figs. 4.05 and 4.06.

Square and cylindrical rods give similar first gaps when they have the same filling fraction near the "QW" case. As the dimensions of the rods increase, and correspondingly the filling fraction, we have complex band structures and at s=0.67 d, we observe as many as three gaps[26] in the same fre-

quency range but these gaps are less important as can be seen by inspection of Table 4.1 and of Fig. 4.06.

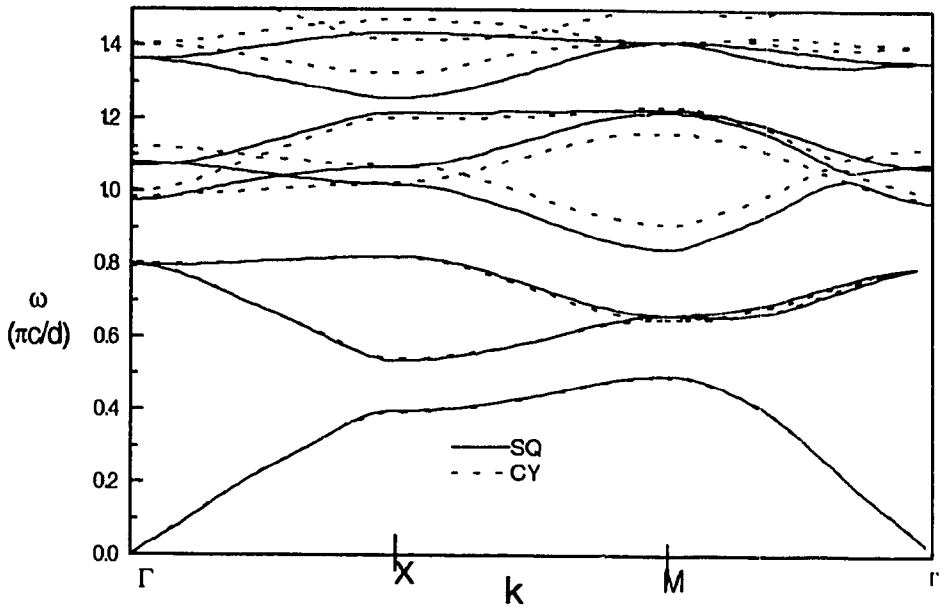

Fig. 4.06 Rods with a square (SQ) or circular (CY) cross section. The parameters are d=1.27cm, s_b=0.85cm(SQ), r_b=0.48cm(CY), ε_a=1, and ε_b=9. Here, the QW condition is not satisfied.

We notice that cylinders and prisms no longer yield the same second and third gaps[40] which are much larger for the cylinders (three and four times larger, respectively). Table 4.01 gives the results for cylinders in a square lattice with an interstitial cylinder per unit. The radius r_b and the dielectric constant ε_b of the main cylinders are equal to 0.48 cm and 9 respectively. The radius r_c and the dielectric constant ε_c of the interstitial rod vary. A very strong interstitial structure

(in dielectric constant or in dimensions) annihilates or strongly diminishes the first gap, but for gaps of higher order the relative width can decrease or increase.

Main rods	Interstial rods	1st gap	2nd gap	3rd gap
r_b	r_c, ε_c	ω_1, $\Delta\omega_1/\omega_1$	ω_2, $\Delta\omega_2/\omega$, $\varepsilon_{b\,2}$	ω_3, $\Delta\omega_3/\omega_3$
0.48cm, 9	no rod	0.527, 9.6%	0.867, 10.9%	1.28, 7.4%
0.48cm, 9	0.24 cm, 9	no gap	0.926, 11%	1.26, 3.95%
0.48 cm, 9	0.24 cm, 4	0.502, 3%	no gap	1.35, 6.1%
0.48 cm, 9	0.12 cm, 9	0.509, 5.9%	no gap	1.33, 9%

Table 4.01. Midgap frequencies and relative gaps for cylindrical rods. The main rods are at the corners and the interstitial ones are at the center of the square units.

The experimental gaps[26] for the case without interstitial cylinders have a relative width equal to 15% for the second midgap (0.87) in the (1,0) direction for only 172 cylinders; the corresponding calculations (Fig. 4.06) for an infinite number of cylinders give 28% and 0,885 respectively.

Let us go back to the rods with a square cross section in square lattices. When we introduce an interstitial rod at the center of the unit cell, the second curve of Fig. 4.05 seems to lower down and gives rise to two full gaps in the

cases when the dielectric constant of the added prism is low (ε=4) or the dimensions are small (s_c=0.5s_b), as shown in Figs. 4.07 and 4.08.

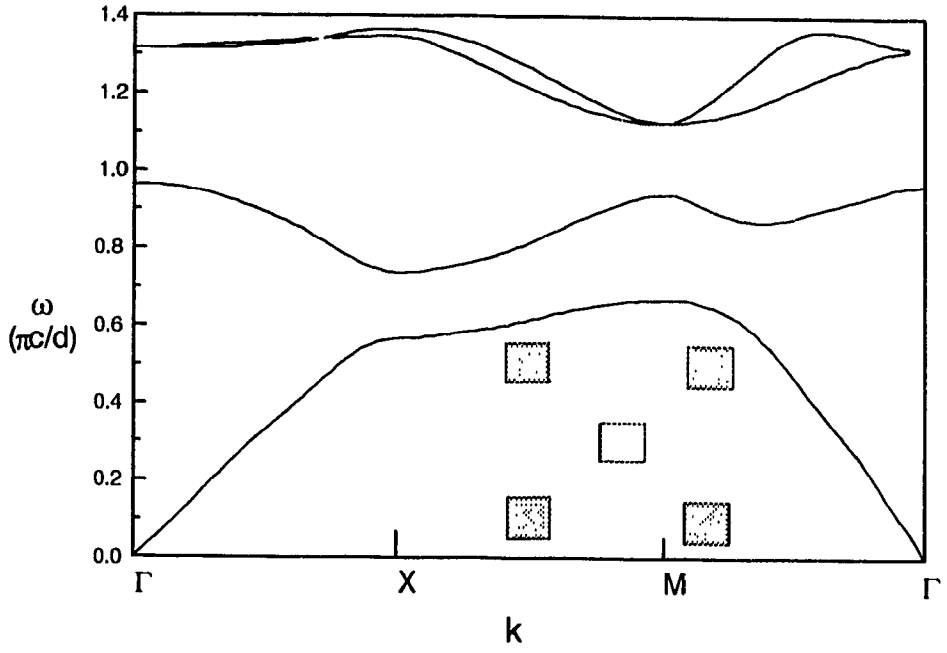

Fig. 4.07. Interstitial rod at the center of the unit cell. The parameters are d=1.27cm, s_b=s_c=0.42cm, ε_b=9, ε_c=4, and ε_a=1.

For the first case, the midgaps are located, respectively, at 0.703 and 1.13 with relative widths of 9.7% and 15.7 %; the corresponding values in the second case are 0.72 and 1.06 and the relative widths 14% and 15 %. We recall that, if the interstitial rod is absent there is only one unmodulated gap at this frequency range with a midgap at 0.79 and a relative width of 30%, cf. Fig. 4.04.

When the interstitial rods are on the axes, as shown in Fig. 4.09, the second and the third curves move together. The filling fraction being larger, we

expect the gaps to be smaller than those of Fig. 4.06. Indeed, this is the case, the first gap is centered at 0.755 and has a relative width of 6 %, whereas the second midgap is centered at 1.247 with a relative width of 1.4%. When the

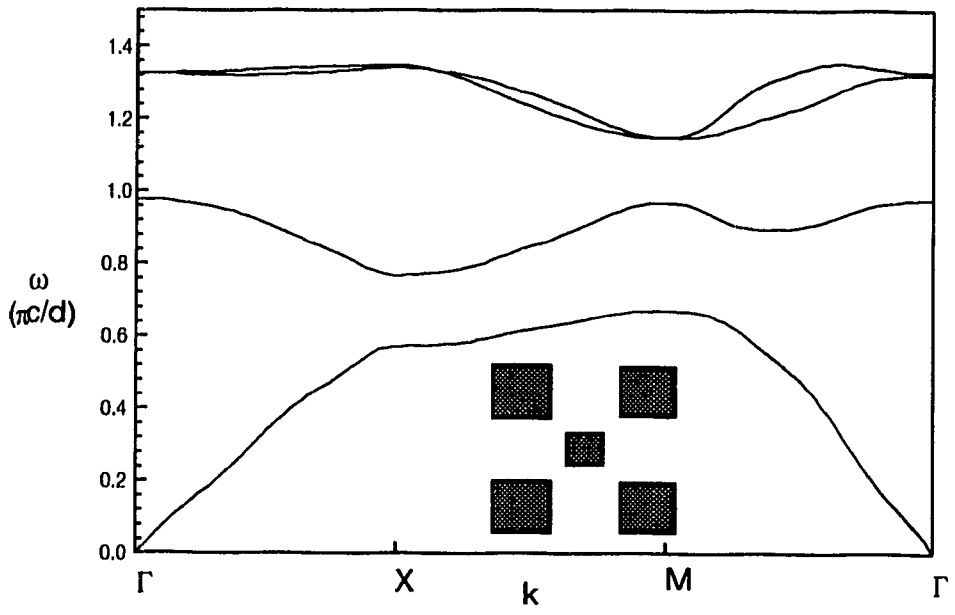

Fig. 4.08. Small intersticial rod at the center of the square. The parameters are d=1.27cm, s_b=0.42cm, s_c=0.21cm, $\varepsilon_b=\varepsilon_c$=9, and ε_a=1.

sides of the extra rods are equal to one quarter of the main rods' sides, we have a picture very similar to that of Fig. 4.06, but the full gap in this interval is a little smaller, 24% instead of 30%. When the filling fraction is large enough, the second curve joins the first and the first gap disappears.

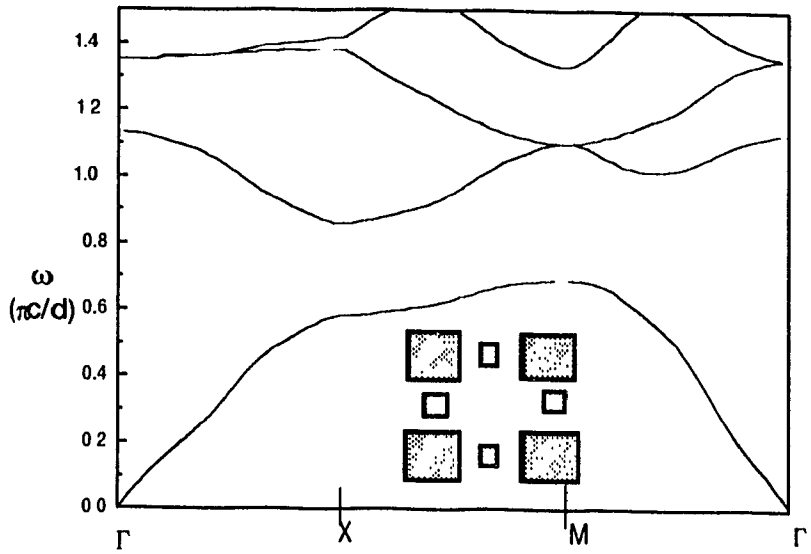

Fig 4.09. Small interstitial rods on the axes. The parameters are d=1.27cm, s_b=0.42cm, s_c=0.21cm, ε_a=1, ε_b=9, and ε_c=4.

Fig. 4.10 shows the case where all the rods have the same dimensions with different dielectric constants. Only the first gap survives with a midgap equal to 0.745 and a relative width $\Delta\omega/\omega$ equal to 1%. If the added rods have the same dielectric constant as the regular ones, the only gap that does not vanish is situated between the second and the third curves, and it has as midgap value 0.91 and a relative width of 3.6%.

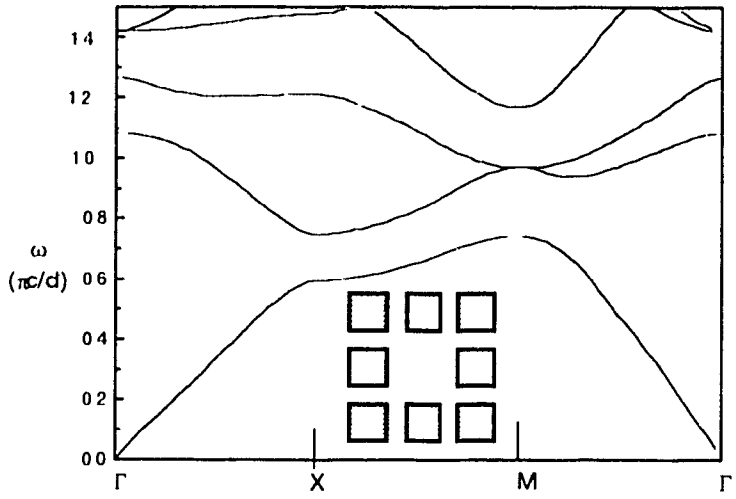

Fig. 4.10. Rods on the axes, with the same size as the main rods. The parameters are d=1.27cm, s_b=s_c=0.42cm, ε_b=9, ε_c=4, and ε_a=1.

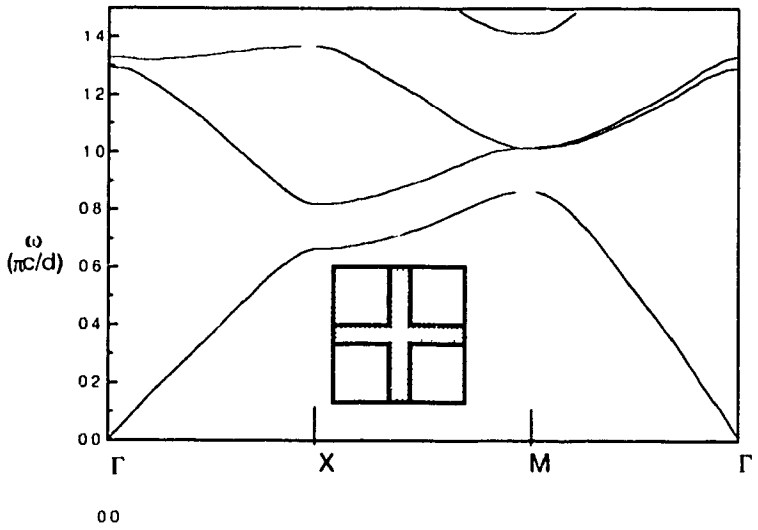

Fig. 4.11. Low-index rods in high-index background. The optical areas are equal. The parameters are d=1.27cm, s_b=1.207cm, ε_a=9, and ε_b=1.

When the dielectric constant of the rods is inferior to that of the background, the situation is quite different even if the product "dielectric constant * cross section" is the same as in the case of the first largest gap above. If styrofoam rods (or air , similar dielectric constant) are placed in a silica composite background at the lattice vectors, the first midgap is at 1.39 and the width 1.6% as shown in Fig. 4.11.

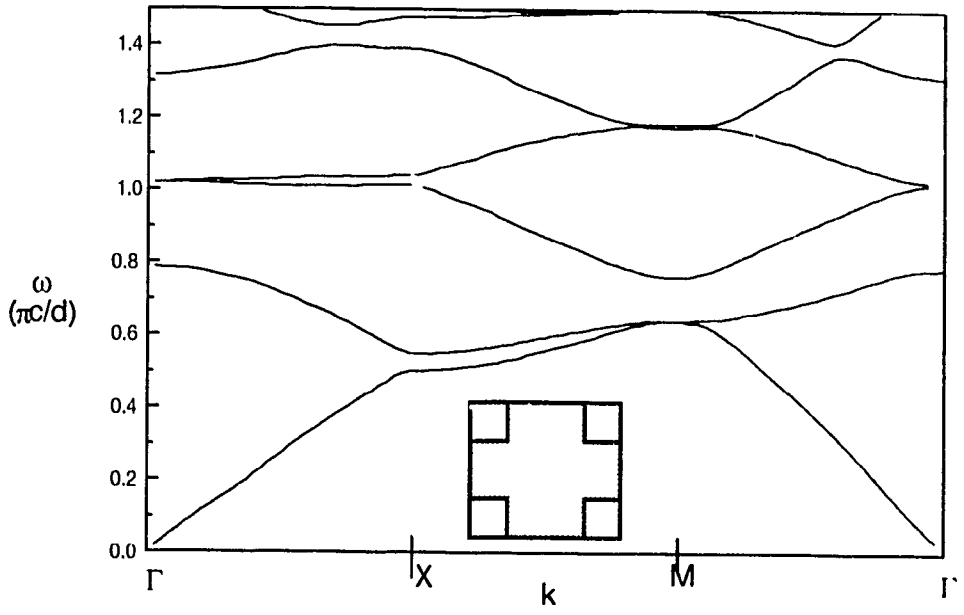

Fig. 4.12 Low index rods in high index background, f=0.45. The parameters are d=1.27cm, s_b=0.42cm, ε_a=9, and ε_b=1.

For a filling fraction f=45%, instead of the 90% used in Fig. 4.11, the situation is no better, the first midgap is around 1.4 and the width 0.5 %.

In this chapter, the plane wave method has been used to find the variation of the TE photonic gaps in 2D structures when extra rods are added. The largest gaps are obtained when high dielectric rods are placed in a low dielectric constant background, and the product "dielectric constant * cross section area" is the same. This is the equivalent of a 1D QW structure. The next chapter gives the conclusions.

Chapter 5

CONCLUSIONS

In the first part of this study, we have outlined the general transfer-matrix method used to describe the propagation of the electromagnetic waves in 1D superlattices. This method is based on matching the solutions of Maxwell's equations at the interfaces. The transfer matrices express the change that the TE and TM electromagnetic wave undergo when they pass through just one periodic unit. They were found analytically for two, three and four-layered units. In physical situations, the electromagnetic field must be finite. This imposes a limit to the eigenvalues of the transfer matrix and the frequencies that give values which are out of range, and therefore are forbidden, giving rise to photonic band gaps.

Starting from the QW structures that have the largest regularly spaced odd gaps when the incident wave is normal to the interfaces, we have found that non QW structures exhibit even gaps. At angles different from the normal, the gap picture is different for TE waves and TM waves, odd and even gaps exist for all structures, with always a total absence of gaps at the Brewster's angle for TM waves.

The introduction of an extra layer in one QW layer shows even and odd bands even for the normal incidence. From this point of view, the situation is the same as for non QW structure. Still, the TM waves do not exhibit any gap at Brewster's angle.

The variation of the gap width has also been studied for normal incidence, when one layer of a two-layered unit changes its width at the expense of the other one. Maxima have been found when the optical widths of the layers are odd multiples of one another.

The effect of the change in position, index and dimension of the extra layer in a four-layered unit on the gap width has been investigated. The second gap increases and the first decreases linearly with the index. The width of the gap varies symmetrically with the position of the extra layer. As a function of this position, the second gap width resembles a quadratic function turned downwards with a maximum reaching 162 % of the QW value. In contrast, the first gap resembles a shallower and upward oriented parabola with a minimum of 43% the QW value. The increase of the extra layer's width leads to a decrease of the first gap width; while other gaps will either increase or decrease.

An anti-reflection layer keeps equal odd gaps while it introduces even gaps in a two-layered structure.

The second part of this thesis deals with 1D finite structures and transmittance. The extent one has to go to, in order to get almost the same results as

those of a 1D infinite structure has been evaluated. Any number of units larger than fifty is sufficient but for three-layered structures with an antireflection layer we need more units to show a total reflection at the even gap frequencies. Missing layers have been found to introduce very narrow minibands in the main gap and Fibonacci chains have a peculiar transmittance pattern that the ratio between the number of different layers cannot explain.

The last part of the thesis treats 2D infinite periodic structures using the plane-wave method. The equivalent of a 2D QW, that is to say, a constant optical path (surface times dielectric constant), still yields the largest gap when the rods have the higher index, ($\Delta\omega/\omega$ superior to 30%). The dimensions of the rods have been changed and more gaps were introduced in the same frequency interval. Extra structures on the diagonal or on the axes reduced the first gap or divided it into two parts while the dimension or the dielectric constant have been found to be less important than their product. The same thing can be said about the general form of the rods. Near the "QW" configuration, cylindrical and square rods yield essentially the same gap pattern, provided their base areas and their dielectric constants are the same. A gap can disappear in a certain frequency interval if the dimensions of the rods are changed or if interstitial rods are introduced.

5.2 Possible applications and further study fields

The main application up to date of the periodic structures is the Bragg reflection in semiconductor lasers. A well tuned Bragg reflector can eliminate undesired frequencies from the lasing cavity and greatly reflect the most usefull ones. 1D, 2D, and 3D Bragg reflectors can be used as mirrors for 1D and 2D laser diode arrays with more convenience than coating[6, 41]. Thresholdless lasers derived from the elimination of non lasing energy will make possible a further miniaturization and integration of low energy lasers.

Spontaneous light emission has been investigated when gaps are present[9]. The frequency selection is easier[43, 27] and the control of the gap frequencies can help.

The separation of TM and TE waves could be carried out in 1D structures because they don't have gaps at the same frequencies when the angle of incidence is different from the normal. As for 2D structures, TM and TE gaps always occur at different frequencies. This would be a possible way to polarize light.

In a further research project, a finite 2D periodic structure could be studied with the scattering method in order to see if transmission is larger in certain directions. The method suggested by Sigalas et al.[34] yields results for the transmission only in one direction and the limits of the periodic arrangement of the rods are not specified.

Still an other aspect of tunability of photonic gaps in 2D periodic structures that can be studied , is the case of the cylindrical and spherical symmetry[5] and extra structures (embedded shells) .

Finally, one can study the transmission of electromagnetic waves emitted by a special antenna through periodic media.

REFERENCES

1 F. Abelès, *Ann. de Phys.*, **3**, 504(1948)

2 M. A. Afromowitz, *Sol. Stat. Com.*, **15**, 59(1974)

3 N. W. Ashcroft, N. D. Mermin, *Solid State Physics*, W. B. Saunders, Orlando, (1976)

4 M. Born, E. Wolf, *Principles of optics*, 6th ed., Pergamon Press, Oxford (1980)

5 D. Brady, G. Papen and J. E. Sipe, *J.Opt.Soc.Am.* B, **10**,644 (1993)

6 D. L. Bullock, S. Chung-Ching and R. S. Margulies, *J.Opt.Soc.Am.* B, **10**, 399 (1993)

7 F. de Martini, G. R. Jacobovitz, *Phys. Rev. Lett.*, **60**, 1711(1988)

8 E. N. Economou, M. Sigalas, in "*Photonic Band Structure and Localization*", edited by C. M. Soukoulis, Plenum Press, New York, 317 (1993)

9 T. Erdogan, K. G. Sullivan, and D. G. Hal, *J.Opt.Soc.Am.* B, **10**, 391 (1993)

10 J. M. Frigerio, J. Rivory, and P .Sheng, *Opt.Com.* **98**, 231(1993)

11 J.D.Gaskill, *Linear Systems, Fourier Transforms and Optics*, Wiley, New York, (1978)

12 W. Gellermann, M. Kohmoto, B. Sutherland, and P. C. Taylor, *Phys.Rev.Let.*, **72**, 633(1994)

13 A. Z. Genack, N. Garcia, *J.Opt.Soc.Am. B*, **10**, 408(1993)

14 O. S. Heavens, *Optical Properties of Thin Films*, Butterworths Scientific Publications, London, (1955)

15 K. M. Ho, C. T. Chan and C. M. Soukoulis, *Phys. Rev. Let.*, **65**, 3152 (1990)

16 J. D. Jackson, *Classical Electrodynamics*, Wiley, New York, (1975)

17 C. Janot, *Quasicrystals, a Primer*, Clarendon Press, Oxford, (1992)

18 B. P. Jeffryes, *Phys.Rev.Let.*, **71**, 1119(1993)

19 D. Kossel, *J.Opt.Soc.Am. B*, 56 ,1434(1966)

20 K. M. Leung, *J.Opt.Soc.Am. B*, **10**, 303(1993)

21 K. M. Leung and Y. F. Liu, *Phys.Rev.Let.*, **65**, 2646(1990)

22 K. M. Leung, in "*Photonic Band Structure and Localization*", edited by C. M. Soukoulis, Plenum Press, New York, 269 (1993)

23 A. A. Maradudin, A. R. McGurn, *J.Opt.Soc.Am.B,* **10**, 307(1993)

24 R. D. Meade, A. M. Rappe, K. D. Brommer and J. D. Joannopoulos, *J.opt.Soc.Am. B,* **10**, 328(1993)

25 E. Merzbacher, *Quantum Mechanics*, Wiley, New York, (1970)

26 S. L. McCall, P. M. Platzman, R. Dalichaouch, D. Smith, and S. Schultz, *Phys.Rev. Let.*, **67**, 2017(1991)

27 T. W. Mossberg and M. Lewenstein, *J.Opt.Soc.Am.* B, **10** , 340, (1993)

28 F. M. Peeters, P. Vasilopoulos, *Appl. phys. Lett.*, **55**, 1106(1989)

29 F. K. Reinhart, R. A. Logan, and C. V. Shank, *Appl. Phys. Lett.* 27, **45** (1975)

30 W. M. Robertson, G. Arjavalingam, R. D. Meade, K. D. Brommer, A. M. Rappe and J. D. Johannopoulos, *J.Opt.Soc.Am.* B, **10**, 322 (1993)

31 S. John, , *Physics Today*, p.32 May (1991)

32 S. John, *Phys.Rev.Let.*, ***58***,1486(1987)

33 S. Schultz and D. R. Smith, in *Photonic Band Gaps and Local ization*, edited by C.M.Soukoulis, Plenum Press, New York, 305, (1993)

34 M. Sigalas, C. M. Soukoulis, E. N. Economou, C. T.Chan, and K. M. Ho , *Phys. Rev. B*, **48**, 14121(1993)

35 D.R. Smith, R. Dalichaouch, N. Kroll, S. Schultz, S. L.McCall and P. M. Platzman, *J.Opt. Soc.Am.* B, **10**, 314(1993)

36 H. S. Sözüer and J. W. Hans, *J. Opt. Soc. Am. B*, **10**, 296(1993)

37 P. Vasilopoulos, F. M. Peeters, D. Ait El Habti, Phys.Rev.B, **41**, (1990)

38 J. T. Verdeyev, *Laser Electronics 2nd ed.*, Prentice Hall, Englewood Cliffs, (1989)

39 P. R.Villeneuve and M. Piché, *Phys. Rev. B*, **46**, 4969 (1992)

40 P.R. Villeneuve and M.Piché, *Phys. Rev. B*, **46**, 4969 (1992)

41 C. C. Weisbuch, B. Vinter, *Quantum semiconductor structures*, Academic Press, Boston (1991)

42 E.Yablonovitch, in *Photonic Band Gaps and Localization*, edited by C. M. Soukoulis, Plenum Press, New York (1993)

43 E. Yablonovitch, *Phys. Rev. Let.*, **58**, 2059(1987)

44 E.Yablonovitch, *J.Opt.Soc.Am. B*, ***10***, 283(1993)

45 A. Yariv, P. Yeh, *Optical waves in Crystals*, Wiley, New York (1984)

46 P. Yeh, A.Yariv, and C.-S. Hong, *J. Opt. Soc. Am.*, **67**, 423 (1977)

47 Z. Zhang and S. Satpathi, *Phys.Rev.Let.*, **65**, 2650(1990).

48 J. P. van der Ziel and M. Ilegems, *Applied Optics*, **14**, 2627 (1975)

49 C. M. Soukoulis, E. N. Economou, G. S, Grest, and M. H. Cohen, Phys. Rev. Lett., **65**, 575(1989)

50 N. Holonyak, Jr., R. Kolbas, R. D. Dupris, and P. D. Dapkus, *IEEE J. of Quant. Electron.* **QE-16**, 170(1980)

51 M. R. Spiegel, *Mathematical handbook*, McGraw-Hill, New York (1968)

52 D. C. Champeney, *Fourier transforms and their physical applications*, Academic Press, London (1973)

53 P. R. Villeneuve, M. Piché, in *Photonic Band Gaps and Localization*, edited by C. M. Soukoulis, Plenum Press, New York (1993)

54 W. H. Press, B. P. Flannery, S. A. Tenkolsky, and W. T. Vetterling, *Numerical recipes*, Cambridge University Press, Cambridge, (1986).

APPENDIX

The programs used in plotting the figures derive directly from the formulae in the text. For the figures in chapter 2, Eqs. 2.15 through 2.18 are used to find the transfer matrix elements. These equations are more flexible than Eqs. 2.22 to 2.27 because we can change more easily the number of layers per unit, and keep the remainder of the program intact. Matrix multiplications are automatically carried out by the program. All the programs in chapters 2 and 3 are built around the same subroutines giving the transfer matrix. The triangular index profile is approximated by 20 small layers with gradual refractive indices.

The transmittances in the third chapter suppose that the media surrounding the structure have the same refractive index as the first layer. The same calculations can be made with the air or the vacuum acting as the input and output media. The gaps will be centered at the same frequencies but they will be larger. The calculations can be carried out by considering one large unit with 34, 68 or 100 layers, the results are the same as if we use Eq. 3.04.

The figures in the fourth chapter are plotted from results obtained with the evaluation of the determinants of matrices shown in Eqs. 4.25 and 4.26. The dimensions of those matrices were limited to 49x49. As the calculations are quite heavy and there is no way to guess where the roots are, the simplest method is used: when the determinant undergoes a sign change, we consider

that the last value of the frequency is a root. When we compare the results obtained with 81x81 matrices to those obtained with 49x49 matrices at chosen frequencies, we conclude that our results are precise up to 3 significant figures. The determination of the matrices determinants were done with a routine found in a numerical recipes book[54], but the calculations were still highly CPU time consuming. A figure such as that of Fig. 4.07 would take 100 minutes of vax2 CPU time with 49x49 matrices, 61x61 matrices would take 160 minutes and 81x81 would take more than 6 hours. Combined to the low priority we had on that machine, we could wait for days before we could analyze the effect of a change on a given structure. The situation was not better on Alcor, the machine is slower, and to make things worse, the working session must be open all the time your program is running: it does not carry out any batch jobs after you have logged off.

Despite of those difficulties, we were able to find results that were similar to those found in the literature[26].